Western University

Scholarship@Western

Electronic Thesis and Dissertation Repository

12-18-2013 12:00 AM

Characterization of the Alternative Oxidase from the Psychrophilic Green Alga Chlamydomonas sp. UWO241

Michael SJ Inman, *The University of Western Ontario*

Supervisor: Dr. Denis Maxwell, *The University of Western Ontario*
A thesis submitted in partial fulfillment of the requirements for the Master of Science degree in Biology
© Michael SJ Inman 2013

Follow this and additional works at: https://ir.lib.uwo.ca/etd

Recommended Citation

CHARACTERIZATION OF THE ALTERNATIVE OXIDASE FROM THE
PSYCHROPHILIC GREEN ALGA *CHLAMYDOMONAS SP.* UWO241

(Thesis format: Monograph)

By

Michael Stewart John <u>Inman</u>

Graduate Program in Biology

A thesis submitted in partial fulfillment
of the requirements for the degree of
Master of Science

The School of Graduate and Postdoctoral Studies
Western University
London, Ontario, Canada

Abstract

The alternative oxidase (AOX) was studied in the psychrophilic green alga *Chlamydomonas sp*. UWO241. AOX is the sole component of the alternative pathway of mitochondrial electron transport and is present in all plant and algal species. *In silico* analysis of the deduced protein sequence of the cloned *AOX* cDNA showed that the UWO241 protein has lower amounts of proline and higher amounts of lysine and tryptophan compared to the AOX sequence of the mesophilic alga *C. reinhardtii*. These changes have been seen in other studies of cold-adapted enzymes. Interestingly, unlike *C. reinhardtii*, AOX transcript abundance in UWO241 did not increase in response to a shift from ammonium to nitrate growth media or to treatment with hydrogen peroxide. A polyclonal antibody that recognizes AOX in *C. reinhardtii* did not cross-react with AOX from UWO241. This finding is consistent with the UWO241 protein being structurally distinct, highlighting its adaptation to low temperature.

Keywords

Acknowledgements

The completion of this work would not have been possible without the supervision of Dr. Denis Maxwell. His constant support and guidance through the scientific process has been invaluable. His words of wisdom and candor were the driving force in my perseverance throughout my first-hand experience with the challenges of academia, and for that I am very grateful.

My advisors Dr. Norm Hüner and Dr. Rob Cumming were consistent sources of inspiration and thoughtful critique. Their guidance through the completion of this work was much appreciated.

My laboratory research would not have been possible without the expertise amassed from the members of the Maxwell lab. Marc Possmayer and Sundaram Pakkiriswami have been invaluable sources of methodological know-how and conversation regarding all things algae, and cricket. Marc's efforts in the creation of the UWO241 cDNA library, as well as his help with experimental techniques greatly aided my own efforts with UWO241. Sundaram's technical knowledge of immunoblotting and AOX were also much appreciated.

My colleagues on the fourth floor of NCB have been a constant and cheery source of knowledge. The Hüner lab in particular was of great help when my many challenges arose and great minds were needed to find solutions.

For instilling a sense of curiosity and wonder in me from a young age, my parents ultimately deserve the greatest proportion of my thanks and admiration. For all of the knowledge and experience I have accumulated, I am at a loss for words to thank you for your love and generosity throughout my life and experience as a student.

Through all the challenges of my graduate degree, one person has stood by my side as a source of unwavering friendship and support. To my wife Sherry, I cannot thank you enough – it's very clear, our love is here to stay.

Table of Contents

List of Figures

List of Appendices

1 Introduction

1.1 The adaptations of psychrophiles

As a harbinger of life, the Earth is a cold place. More than 80% of the Earth's surface is permanently below 5°C, which includes the majority of deep sea water that has an average temperature of 2°C (Russell 1990). From a moderate climate dwelling, endothermic, animal species perspective, the prospect of finding life in these seemingly inhospitable environments seems unlikely. And yet organisms representing each domain of life are found in these widespread cold environments. The growth of organisms within these cold environments, and in fact throughout the biosphere, is dependent on their ability to maintain high rates of metabolic processes that are driven by temperature-sensitive enzymatic reactions. Therefore the biology of cold-adapted organisms has been investigated to understand how biochemical reactions are catalyzed by enzymes under cold conditions.

Many microbes that grow in permanently cold environments are defined as psychrophilic because they possess two specific traits: (i) they have a maximum growth temperature below 16°C, and (ii) they are unable to grow at temperatures above 20°C (Morita 1975). In contrast to psychrophiles, the majority of ectotherms are classified as mesophilic because they have an optimum temperature for growth between 25 and 45°C (Brock 1985). Some mesophilic organisms are able to grow at temperatures below 16°C, even though their optimal growth temperature lies between 25 and 45°C, but these organisms are considered cold-tolerant. The third class of organisms, grouped according to their optimum growth temperature, are termed thermophilic, which are able to grow and reproduce at temperatures between 60 and 80°C. Some species of thermophilic archea have been observed at a growth temperature of 113°C (see Rothschild and Mancinelli 2001).

From a purely thermodynamic perspective, growth and reproduction at low temperatures represents a significant challenge, and yet a wide range of ectotherms are seemingly well adapted to cold climates. For example, some algae and diatoms excrete polysaccharides and other small molecules into the surrounding snow in order to create pockets of liquid water – a process that allows for metabolic activity to occur (Raymond et al. 1994, Pikuta et al. 2007).

Research on a diverse array of cold-adapted organisms have shown they possess distinct differences in structure and function of a range of cellular processes when compared to organisms adapted to moderate temperatures. There has been considerable research investigating the underlying biochemical and physiological differences that account for the ability of an organism to adapt to a specific temperature niche. Most research has focused on two fundamental aspects of cellular biochemistry that are known to change with temperature: the rate of enzyme-catalyzed reactions (Siddiqui and Cavicchioli 2006), and membrane fluidity (Russell 1997).

The rate of a chemical reaction or an enzyme catalyzed reaction can be described by a modified form of the Arrhenius equation: $k_{cat}=A\kappa e^{-Ea/RT}$. This equation states that the rate constant for an enzymatic reaction of a known concentration of enzyme (k_{cat}) is dependent on the activation energy (E_a) and the absolute temperature of the reaction (T) (the remaining values are constants: A is the preexponential factor, κ is the dynamic transmission coefficient, and R is the universal gas constant) (see Siddiqui and Cavicchioli 2006). The calculated value of $e^{-Ea/RT}$ represents the proportion of enzyme molecules that contain the minimum energy required to catalyze a reaction.

Given that the number of enzymes able to meet the minimum energy requirements to carry out a reaction is generally thought to decrease exponentially with temperature, how do psychrophilic organisms maintain appreciable reaction rates at temperatures around 0°C? One adaptation observed in psychrophilic bacteria is the increased production of enzymes in order to compensate for the low rates of reaction at cold temperatures (Feller et al. 1990). To prevent the need to increase concentrations of all enzymes, cold-adapted organisms have adapted the means to modify enzyme catalytic activity through specific changes in primary protein structure (Margesin and Schinner 1994).

The current model explaining the activity of psychrophilic proteins posits specific modifications within the amino acid structure in order to modify the reaction rates of certain enzymes. The substitutions in primary protein structure that seem to allow for the increased flexibility of cold-adapted enzymes include: a greater number of amino acids with aromatic side chains, a reduction of proline, the reduction of bulky side chains surrounding the active site, and in some cases a change in the polarity of side chains to facilitate a change in

electrostatic potential (Feller and Gerday 2003). These modifications would allow for a change in the optimal temperature, whereby the amount of energy available at temperatures below 5°C would be sufficient to drive an enzymatic process, and therefore the metabolic processes required for life (Siddiqui and Cavicchioli 2006).

Changes to the primary sequence of a number of enzymes have been investigated in both eukaryotic and prokaryotic cold-adapted microbes (Russell et al. 1998; Devos et al. 1998). Compared to phylogenetically close mesophilic counterparts, all of these enzymes display amino acid substitutions. In fact, the variation in amino acid composition between mesophiles and psychrophiles has been quantified through a comparison of the proteomes of several species. When examined on a whole, the proteome of cold-adapted organisms appears to preferentially substitute certain amino acids in favour of residues that contribute to conformational flexibility and therefore high activity at low temperatures (Metpally and Reddy 2009).

The observed structural differences of psychrophilic enzymes have led to the widely accepted concept of greater protein flexibility in cold-adapted enzymes. This concept has been experimentally investigated in the α-amylase enzyme from psychrophilic, mesophilic, and thermophilic sources. The conclusion of this analysis has shown that cold-adapted enzymes are more permeable to fluorescence quenching molecules that bind to tryptophan, an observation that is hypothesized to occur due to greater accessibility of the substrate to the catalytic site (D'Amico et al. 2003). An investigation of the citrate synthase of an Antarctic bacterium (DS2-3R) by Russell et al. (1998) also demonstrates this increased binding through measurement of its X-ray crystal structure. The cold-adapted citrate synthase showed a greater accessibility of substrates to the active site through specific modifications to its primary structure. This observation suggests a greater range of conformational states in cold-adapted enzymes, which contributes to their permeability to substrates and, therefore, increased catalytic activity (Russell et al. 1998).

The biological significance of an increase in protein conformational states and therefore flexibility is one of the main contributing factors thought to allow for enzymatic activity at low temperatures, as well as the subsequent loss of psychrophilic protein stability at higher temperatures (see Siddiqui and Cavicchioli 2006). Russell et al. (1998) showed

modifications surrounding the substrate-binding site toward more positively charged residues in order to increase the recognition of a negatively charged substrate.

In addition to the structural modifications that psychrophilic enzymes employ to overcome the limitations of a cold environment, other post-translational modifications may play a role in the alteration of enzyme kinetics at low temperatures. Although most enzymes use post-translational modifications such as phosphorylation in order to facilitate a downstream biochemical reaction, there are several other modifications that may alter the structure or function of a protein. In the context of cold-adapted enzymes, glutathionylation, that is the addition of the tripeptide glutathione to cysteine residues, has been shown to modify proteins such that they can maintain their reduced state even in times of environmental stress (Castellano et al. 2008). One particular modification studied in the psychrophilic bacterium *Pseudoalteromonas haloplanktis* showed that the glutathionylation of its superoxide dismutase resulted in a change in its susceptibility to enzymatic inactivation (Castellano et al. 2008).

1.2 The psychrophilic algae *Chlamydomonas sp.* UWO241

Chlamydomonas sp. UWO241 is an obligate psychrophilic green alga originally isolated from Lake Bonney in Antarctica (Neale and Priscu 1995). Isolated from a depth of 17 m below the perennially ice-covered lake, UWO241 is adapted to low light intensities (about 20 times below ambient), a constant low temperature (1 to 6°C), and high salinity (1.5 M) (Neale and Priscu 1995). UWO241 is a unicellular photoautotroph that contains a single large chloroplast and several mitochondria. It is a diflagellate with a light-sensitive eyespot, which contributes to its phototactic response (Pocock et al. 2004).

Laboratory growth conditions for UWO241 were evaluated, and a growth temperature of 10°C was found to produce a maximal rate of growth (Morgan-Kiss et al. 2006). When UWO241 is shifted to 24°C a lethal response is observed, contributing to its classification as a psychrophile (Figure 1-1) (Possmayer et al. 2011).

Preliminary research with UWO241 has shown that, compared to the related mesophilic green alga *C. reinhardtii*, UWO241 displays a number of differences in its overall physiology, as well as the components and function of its photosynthetic electron transport chain. At the protein level, amino acid shuffling has been observed, specifically the addition of three cysteine residues in the cytochrome *f* protein that do not participate in substrate binding, but appear to contribute to a lower stability at higher temperatures (Morgan-Kiss et al. 2005). In terms of adaptation at the level of lipid biochemistry, higher proportions of unsaturated fatty acids have been observed; specifically, UWO241 has greater amounts of unsaturated fatty acids, which contribute to a higher membrane fluidity and therefore greater permeability of membranes at cold temperatures (Morgan-Kiss et al. 2002).

The current body of evidence of the adaptation of UWO241 to its Antarctic environment has mainly focused on its photosynthetic apparatus. Morgan-Kiss et al. (2002) studied the effect of polyunsaturation of thylakoid membrane lipids on the photosynthetic ability of UWO241 treated with increasing temperature. The adaptation of UWO241 to low intensity and blue-green wavelength enriched light was found to decrease the ability of UWO241 to acclimate to red-light (Morgan-Kiss et al. 2005). Pocock et al. (2011) examined the photosynthetic response and ability of UWO241 to grow in high salt and at low temperature. Szyszka et al. (2007) examined the response of UWO241 under high-light conditions and showed that UWO241 is able to maintain a balance between light-harvesting and excess energy dissipation.

 A detailed study of the response of UWO241 to supra-optimal temperatures was carried out by Possmayer et al. (2011). When shifted from a growth temperature of 10°C to a non-permissive temperature of 24°C, the capacity of UWO241 to undergo photosynthetic and mitochondrial electron transport was reduced. An increase in the mRNA transcript abundance of heat shock proteins *HSP90A* and *HSP22A* was observed upon heat stress. In addition, a reduction in the amount of mRNA transcript for the light harvesting associated polypeptide *LHCBM7*, and the photosynthetic electron transport protein ferredoxin (*FED-1*) was observed. These modifications in transcript abundance under heat stress were reversed upon recovery of UWO241 at 10°C. This indicates that heat stress elicits a disruption to the physiology of
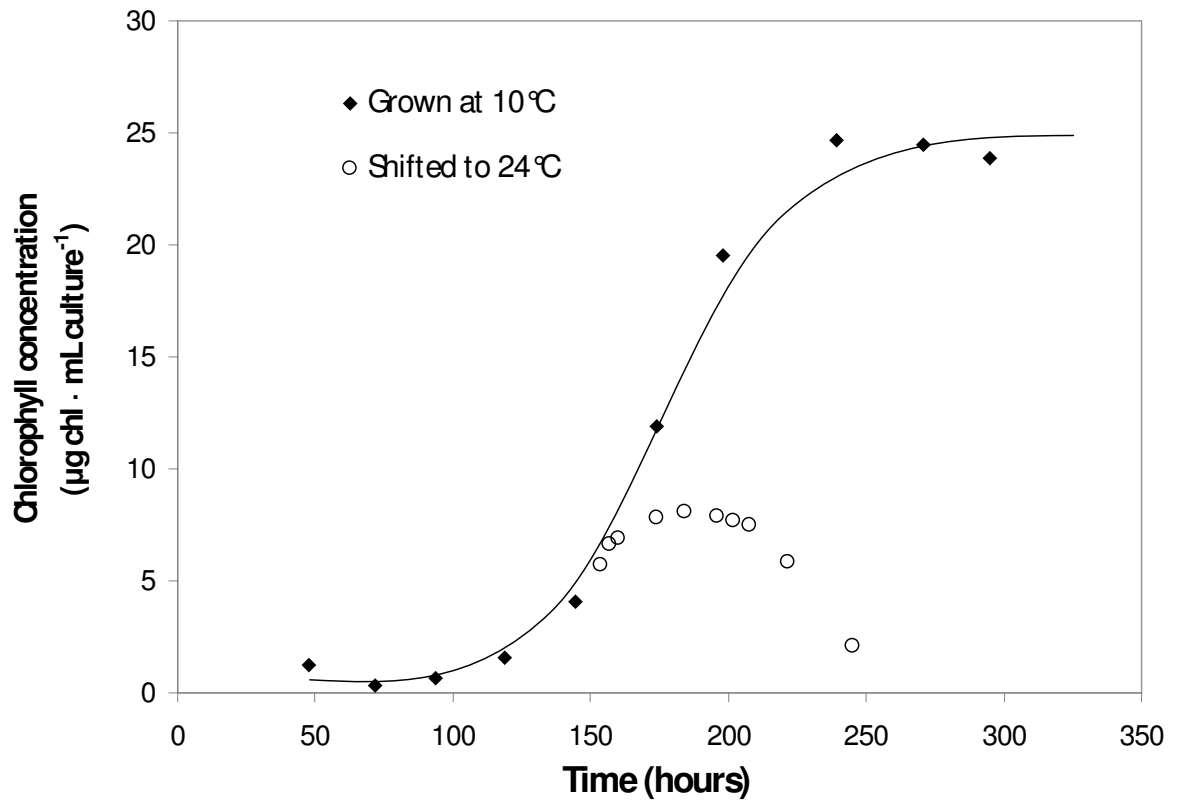
Figure 1- 1Growth of *Chlamydomonas sp.* UWO241 at 10°C and at 24°C.

Growth was measured based on the chlorophyll content of sampled cell cultures beginning 48 hours after inoculation. Adapted from Possmayer et al. (2011)**.**

UWO241. Perhaps more important is the ability of UWO241 to reverse the physiological damage when allowed to recover.

These observations suggests that exposure of UWO241 to 24°C growth conditions initiates a physiological response that is consistent with the reactions observed in other psychrophilic organisms undergoing an acute stress, whereby heat shock proteins are produced to stabilize heat-sensitive proteins (Vayda and Yuan 1994; Deegenaars and Watson 1998).

1.3 Mitochondrial electron transport and the alternative oxidase

UWO241 is typical of many single cell green algae in that it contains a single large chloroplast and one to eight mitochondria (Harris 1989). As in all eukaryotes, mitochondria are the site of the Citric Acid Cycle, which provides a source of reducing equivalents for the capture of chemical energy. The electron transport chain (ETC) within the inner mitochondrial membrane begins with a cytochrome protein complex that oxidizes NADH in order to reduce a pool of ubiquinone (Figure 1-2). This pool of reduced ubiquinone is then oxidized in order to transport electrons further down the cytochrome pathway. The cytochrome complexes facilitate the movement of electrons through the inner mitochondrial membrane, and the movement of protons across the inner membrane, which generates a proton gradient. This proton gradient between the intermembrane space and mitochondrial matrix allows for the production of ATP. The reactions facilitating the transport of electrons through the cytochrome pathway consume oxygen and NADH while producing H_2O and ATP.

In addition to the ubiquitous cytochrome pathway of respiratory electron transport, all plants, algae, and some animal species (McDonald et al. 2009) possess an alternative pathway of respiration. This pathway was originally identified in many plant, algae, moss, and fungi species during a screen for insensitivity to cyanide, the metabolic poison that blocks cytochrome electron transport (Siedow and Berthold 1986). The alternative pathway (AP) contains a nuclear-encoded mitochondrial terminal oxidase protein known as the alternative oxidase (AOX). This di-iron binding protein is the sole component of the so-called
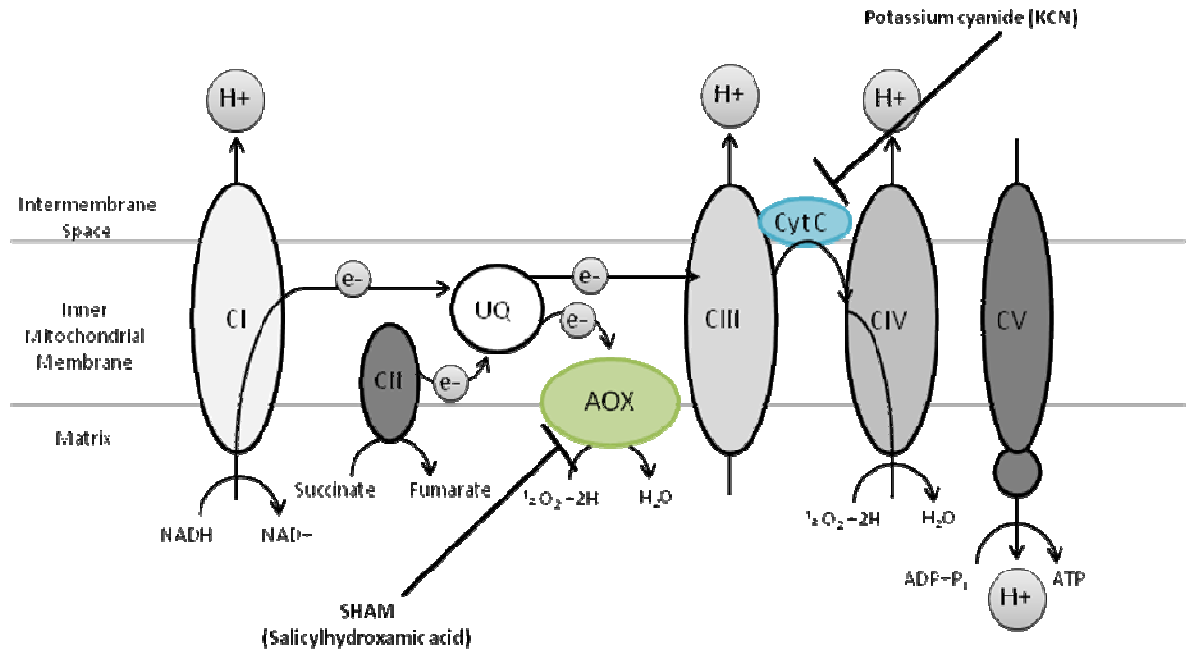
Figure 1- 2 Schematic of the mitochondrial electron transport chain of organisms containing an alternative oxidase (AOX).

The linear flow of electrons through the cytochrome complex proteins NADH dehydrogenase (CI), succinate dehydrogenase (CII), cytochrome bc_1 (CIII), and cytochrome oxidase (CIV) are shown. The proton gradient established by the cytochrome complexes allows for the generation of ATP through ATP synthase (CV). Also shown are the pool of ubiquinol and reduced ubiquinone (UQ), and cytochrome c (Cyt C). Flat head arrows indicate inhibition of AOX and Cyt C by salicylhydroxamic acid (SHAM) and potassium cyanide (KCN), respectively. The alternative pathway of electron transport begins at the pool of ubiquinone which is oxidized by AOX.

alternative pathway that facilitates a four step reaction in which O2 is completely reduced to H2O (Berthold 2000). This alternative pathway dissects the normal flow of electrons through the cytochrome pathway at the point of the ubiquinone pool in times of high oxidative load (Figure 1-2).

1.4 Structure and function of the alternative oxidase

As shown in Figure 1-2, alternative pathway respiration bypasses two of the three sites along the cytochrome chain where electron transport is coupled to proton-pumping. Because of this, AP respiration does not conserve the energy present in substrate molecules and instead the energy is simply dissipated as heat. The increased heat production in mitochondria that have high levels of AP respiration is critical in the flowers of arum species, where it is used to volatilize attractants for pollinators (Meeuse 1975).

To date, the use of AOX in the flowers of arum species is the only definitive function of AOX, and yet it is found universally in all plants, and even species of lower animals (McDonald et al. 2009). Defining a single role for AOX and alternative pathway respiration in non-thermogenic plants and algae has been surprisingly difficult (Vanlerberghe and McIntosh 1997).

In non-thermogenic species, the engagement of AOX has been hypothesized as a mechanism to keep the redox state of the ubiquinone pool from becoming over-reduced. This state may occur when environmental conditions, such as cold, restrict the flow of electrons along the cytcohrome pathway (Vanlerberghe and McIntosh 1992). As well, it may play a role in keeping upstream carbon metabolism of the Citric Acid Cycle operating efficiently when environmental factors such as high light or low temperature create an imbalance in energy metabolism (Noctor et al. 2007).

Maxwell et al. (1999) conclusively showed that transgenic tobacco cells over-expressing AOX had lower levels of mitochondrial reactive oxygen species (ROS) than WT, and cells in which *AOX t*ranscripts were decreased with anti-sense oligonucleotides had appreciably higher levels of ROS. These findings are consistent with AOX playing a key role in regulating the redox state of the ubiquinone pool. Because overproduction of the ubiquinone

pool has been shown to increase mitochondrial ROS formation in plants and protozoan species, it has been suggested that AOX is used to lower the amount of free electrons as a result of a fluctuation in cellular energy requirements (Siedow and Moore 1993).

The amino acid sequence of AOX from many different species has been examined. Conserved residues that contribute to the di-iron binding capacity of AOX have been located in four highly conserved regions: Leu Glu Thr (LET), Asp Glu Arg Met His Leu (NERMHL), Leu Glu X X Ala (LEXXA), and Arg Ala Asp Glu X X His (RADEXXH) (Berthold 2000). These motifs are embedded in several of the helices that comprise the bulk of the structure of AOX and create the reaction centre that facilitates association of two iron atoms, which allows for the reduction of oxygen (Figure 1-3; Albury et al. 2009). The orientation of AOX within the mitochondrial membrane is thought to be interfacial, with the active site facing the matrix (Andersson and Nordlund 1999). This orientation allows for its interaction with the ubiquinol pool in the intermembrane space and oxygen molecules in the matrix.

In all plant species investigated, *AOX* is coded by a multigene family (Vanlerberghe and McIntosh 1997). Different *AOX* genes may be expressed at different developmental stages in soybean (McCabe 1998). Additionally, regulation of AOX has been shown in response to common abiotic factors such as exposure to low temperature in tobacco (Vanlerberghe and McIntosh 1992), or a shift in nitrogen source in *C. reinhardtii* (Molen et al. 2006). The existence of an *AOX* multigene family is not restricted to plants. *C. reinhardtii* contains two *AOX* genes: *AOX1* and *AOX2* (Dinant et al. 2001).

While the AOX proteins of many plants exist as dimers (Umbach and Siedow 1993), there is no evidence that the AOX of unicellular species exist in the same conformation. In fact, a conserved cysteine residue observed in most angiosperms has been suggested as the method of dimerization through disulfide linkage of polypeptides; however, this conserved residue is not observed in unicellular species (McDonald 2009).
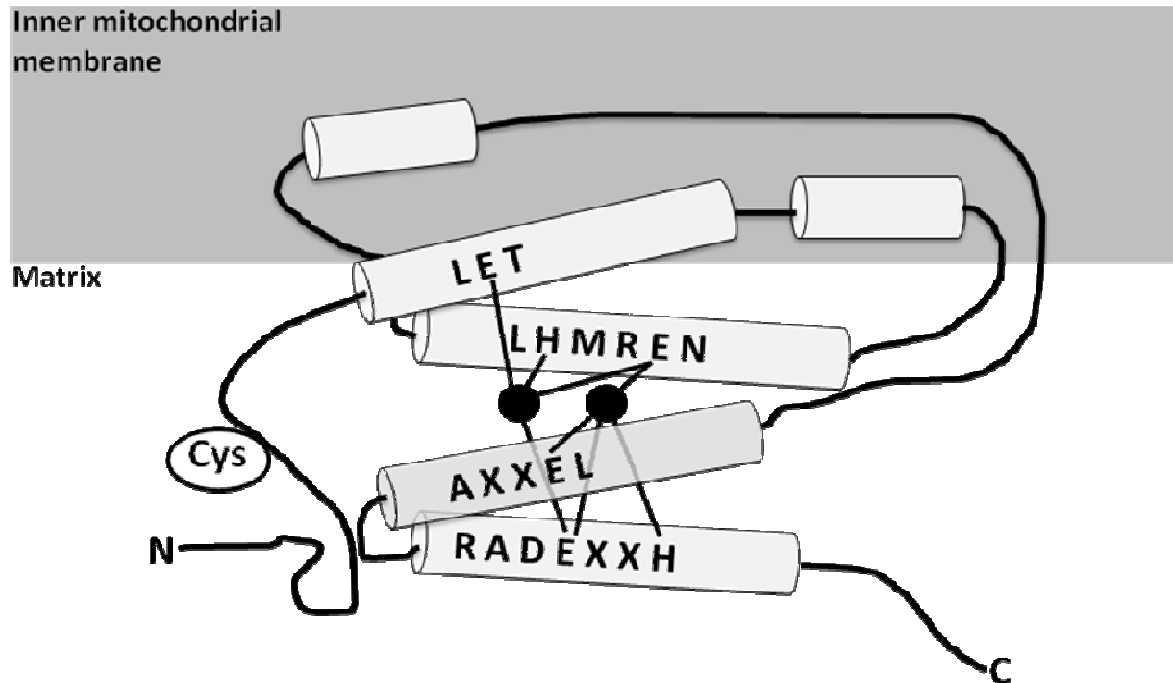
Figure 1- 3 Current understanding of the structure and orientation of the alternative oxidase.

The alternative oxidase is shown as an interfacial protein in the inner mitochondrial membrane. The N- and C-termini of the polypeptide are shown, as well as the location and orientation of secondary structures (cylinders). Conserved amino acids and iron-binding motifs are in bold (LET, NERMHL, LEXXA, and RADEXXH) in their orientation within the secondary structure. A conserved cysteine (Cys) involved in dimerization of AOX is also shown. Black circles indicate iron atoms which are bound to the specific residues involved in iron-binding (Adapted from Albury et al. 2009).

1.5 Thesis objectives

Considering the wealth of information pertaining to AOX in mesophilic organisms, and the lack of information on the enzyme in psychrophilic organisms, the overarching objective of this study is to characterize the AOX of the obligate psychrophile *Chlamydomonas sp.* UWO241. This objective was investigated in conjunction with the mesophilic *Chlamydomonas reinhardtii* 325R. Therefore, the central hypothesis to be tested is whether the psychrophilic alga UWO241 has an alternative oxidase that aligns with known sequences, and yet shows structural and functional divergence from that of *C. reinhardtii*. To that end, the following objectives were investigated:

Objective 1: To isolate the *AOX* cDNA sequence and the deduced AOX protein sequence of UWO241 in order to align these sequences with those of other organisms. This would allow for the analysis of the predicted protein's conserved residues including its AOX antibody binding motif.

Objective 2: To characterize the expression of *AOX* in UWO241 under conditions known to elicit its expression (nitrate, hydrogen peroxide, and temperature) using semi-quantitative RT-PCR, and compare these expression profiles to those of *C. reinhardtii* under the same conditions.

Objective 3: To examine the total mitochondrial, cytochrome, and alternative respiration capacities of the psychrophile in response to different stressors. The ability of *C. reinhardtii* to undergo mitochondrial respiration at cold temperatures will also be examined and compared to UWO241.

An examination of the data obtained from these objectives will give further insight into the physiology and adaptation of UWO241 to an extreme polar environment, and its divergence from the mesophilic *C. reinhardtii*.

2   Materials and Methods

2.1   Strains and growth conditions

Chlamydomonas sp. UWO241 stocks were maintained on agar plates (1.5% w/v) containing high salt (HS) medium, 10 mM sodium chloride, and 15 mM sodium acetate (Sueoka 1960). Stocks of *Chlamydomonas reinhardtii* 325R were maintained on agar plates containing tris acetate phosphate (TAP) medium (Harris 1989). Stocks were inoculated into 250 mL Erlenmeyer flasks containing HS or TAP liquid medium that were kept on a rotary shaker (150 rpm) under constant illumination (80 µmol photons m^{-2} s^{-1}) and constant temperature (5°C or 28°C). Sub-cultures of this liquid stock were used for experimental cultures grown in 300 mL glass tubes submerged in aquaria maintained at 10°C.

In the case of the mesophilic *C. reinhardtii* 325R, sub-cultures were maintained on a rotary shaker in 1L flasks at 28°C under constant illumination (120 µmol photons m^{-2} s^{-1}). In the case of the aquaria-cooled tubes, ambient CO_2 was pumped through 0.2 µm syringe filters and into the tubes as a carbon source, and were under constant illumination from fluorescent lights (120 µmol photons m^{-2} s^{-1}, Sylvania CW-40, Osram-Sylvania, Mississauga, Ont.). Cell cultures in the mid-exponential phase were used for experimentation.

2.2   cDNA library screening, cloning, and alignment of sequence data

A cDNA library for UWO241 was created using a ZAP-cDNA Synthesis Kit (Agilent Technologies, Cedar Creek, TX) from total RNA extracted from cultures grown at 5°C (for RNA extraction protocol see below). The cDNA library was then screened for AOX by using primers of known conserved regions within the *C. reinhardtii* AOX sequence available through the NCBI database (http://www.ncbi.nlm.nih.gov/projects/mapview/map_search.cgi?taxid=3055). Two AOX-specific primers were used to isolate the full length cDNA in concert with two vector-specific primers. The AOX-specific forward primer (primer 037) (5'-TCCTTCGACTGGGTCACCAGCTAC-3'), and reverse primer (primer 012)

(5'-GGGGGCCATCAGGTAGGAGAGG-3') were used with vector-specific primers T7
(5'-TACGACTCACTATAGGGCGAATTG-3'), and T3
(5'-GCTTCCGGCTCGTATGTTGTGTGG-3'), respectively.

High-Fidelity DNA polymerase (Phusion Taq, New England BioLabs, Ipswich MA) was
used in PCR reactions to amplify the AOX sequences from the two primer sets. Samples
were run on a 1% (w/v) agarose gel and stained with ethidium bromide. Bands of the desired
molecular weight were cut out of the gel and purified using a gel extraction kit (Qiagen,
Hilden, Germany). Purified gel extracts were then used for cloning. Extracts were treated
with dATP and Taq polymerase to add a single adenosine overhang. This reaction was then
ligated into a pGEM-T Easy cloning vector and transformed into competent bacterial cells.
 Bacterial cultures were grown on LB agar plates supplemented with 100 µg/mL ampicillin,
0.1 M isopropyl β-D-1-thiogalactopyranoside (IPTG), and 50 µg/mL X-Gal. White colonies
were selected after overnight incubation and grown in liquid LB and ampicillin (100 µg/mL).

Plasmids from transformed colonies were isolated using a QIAprep plasmid isolation kit
(Qiagen, Hilden, Germany) and sent for sequencing reactions (Robarts Research Institute,
London, ON). Vector-specific sequence was removed from sequence data using the
Geneious software (Version 6.0.5) and overlapping gene-specific sequences were condensed
into a single gene sequence.

The nucleotide sequence produced from two clones was used to search for similar sequences
in the National Center for Biotechnology Information (NCBI) website. A discontiguous
megablast with default gap penalties was used to align the unknown sequence with the
Chlamydomonas reinhardtii genome database (Taxonomy ID: 3055). Nucleotide sequence
data were used to generate amino acid sequences that were then aligned with existing AOX
protein sequences available on the NCBI database (http://www.ncbi.nlm.nih.gov).
Alignment values were calculated using the NCBI basic local alignment tool (BLAST) for
protein sequence analysis with default gap cost settings.

A multiple protein sequence alignment was generated using the Clustal X program Version
2.0 with default settings for gap penalties to visualize conserved motifs (Thompson et al.
1997; McDonald 2009). The protein sequences used to generate the alignment included:

Arabidopsis thaliana AOX1a (NP_188876.1), *C. reinhardtii* AOX1 (XP_001694605.1) and AOX2 (XP_001703329.1), *Oryza sativa* AOX (BAA86963), *Glycine max* AOX (CAA48653), *Nicotiana tabacum* AOX (AAC60576.1), and *Volvox carteri* AOX (XP_002955181.1).

2.3 RNA isolation and reverse transcriptase amplification of cDNA

Total RNA was prepared from 50 mL aliquots of cells harvested by centrifugation (5000 × g for five minutes at 4°C) and snap frozen in liquid nitrogen. RNA extraction was performed using a modified cetyl trimethyl ammonium bromide (CTAB) and lithium chloride precipitation method (Untergasser 2008). Briefly, a CTAB buffer supplemented with 1% (w/v) β-mercaptoethanol and 2% (w/v) polyvinylpyrolidone was warmed to 60°C and added to cell pellets. Pellets were warmed to 60°C and vortexed to resuspend in buffer. Two chloroform extractions were performed with centrifugation (16,100 × g) between each extraction followed by addition of isopropanol. After centrifugation, the resulting pellet was washed in 70% ethanol and dissolved in diethylpyrocarbonate (DEPC)-treated dH_2O. Nucleic acids were precipitated using 4 M LiCl following incubation at -20°C. Precipitation of polysaccharides was achieved using 3 M sodium acetate (pH 5.2, 1/30th volume) and 100% ethanol (1/10th volume). The nucleic acids remaining in the supernatant were precipitated by the addition of 3 M sodium acetate (1/10th volume) and 100% ethanol (2.5 volumes), and incubated at -20°C overnight. The resulting pellet was washed in 70% ethanol, dissolved in DEPC-treated dH_2O and stored at -20°C.

Total RNA was quantified by spectrophotometric analysis in dH_2O using the A_{260}/A_{280} method (Sambrook and Russell 2001). The nucleic acid concentration is calculated by multiplying the dilution factor and the extinction coefficient of RNA by the spectrophotometric absorbance value at a wavelength of 260 nm. The ratio of the two absorbance wavelengths is used as a measure of nucleic acid purity.

Reverse transcription of total RNA was performed to create a pool of cDNA available for semi-quantitative PCR (sqRT-PCR). Total nucleic acid samples were treated DNase I treated

(1 µg of RNA for sqRT-PCR) according to the manufacturer's instructions to remove genomic DNA (Invitrogen, Life Technologies, Burlington, ON). Reverse transcription of the DNase I-treated RNA pool was performed using Oligo (dT^{12-18}) primers (0.5 µg/mL), dNTP mix (10 mM), dithiothreitol (DTT, 0.1 M), $MgCl_2$ (25 mM), DEPC-treated dH_2O, and SuperScript II reverse transcriptase with its appropriate first strand buffer (Life Technologies, Burlington, ON). A concurrent negative control was performed with each reaction which, received no reverse transcriptase enzyme.

2.4   Heat stress, nitrate, and hydrogen peroxide treatments, and semi-quantitative PCR

Cultures of UWO241 were put under heat stress by moving culture tubes into preheated aquaria. UWO241 cultures grown at 10°C were shifted to 24°C. Aliquots of cells were sampled 0, 3, 12, 24, and 48 hours after being shifted to heated aquaria. Samples were collected by centrifugation and snap frozen in liquid nitrogen. Total RNA was extracted as described in section 2.3, and 1 µg of RNA was reverse transcribed to be used for sqRT-PCR. Cultures of 325R were grown to mid-log phase in 28ºC shakers and then moved to a shaker preheated to 40ºC.

AOX mRNA transcript abundance was measured using primers previously used for UWO241 cDNA library screening (primers 012, and 037). Primers for the D1 and D2 domains of the large ribosomal subunit rDNA were used as a loading control (primer NL1: 5'-GCATATCAATAAGCGGAGGAAAAG-3', and primer NL4: 5'-GGTCCGTGTTTCAAGACGG-3'). Primers for AOX expression in 325R were forward primer 001: 5'-CCTAGGCACGGCAGTATGAC-3' and reverse primer 002: 5'-CATTACACTTTTCTCCAGACA-3'. Primers for the 18S ribosomal DNA subunit were used as a loading control (forward 5'-GTAGTCATATGCTTGTCTC-3' and reverse 5'-GGCTGCTGGCACCAGACTTGC-3') for 325R sqRT-PCR.

Optimization of PCR cycle number was performed to determine when reactions were in exponential phase for each set of primers (Appendix A). All ethidium bromide-stained gels were visualized using a BioRad Gel Doc and quantified using the Quantity One software (Version 4.5.1, Bio-Rad Laboratories Canada Ltd., Mississauga, ON). This quantification

method uses an adjusted volume analysis based on the saturation of pixels for a certain area in a digital image of the gel. The adjusted volumes of AOX signal were then corrected using the values from the loading control in order to produce a relative value for each sample. At least three technical replicates were run for each series of treatments, and the standard error was calculated for each time point using Microsoft Excel.

2.5   Protein isolation and immunoblotting

Total soluble proteins were isolated from 50 mL aliquots of cells, collected into a pellet by centrifugation (5000 × g). Cell pellets were dissolved in a commercial protein extraction buffer (Agrisera AS08 300, Vännäs, Sweden) containing glycerol (40% v/v), Tris-HCl (pH 8.5), LDS (lithium dodecyl sulphate), and EDTA (ethylenediaminetetraacetic acid), which was mixed with a protease inhibitor (Roche Diagnostics Corporation, Indianapolis, IN) dissolved in Tris-HCl (20 mM, pH 7.2) and EDTA (0.1 µM, pH 8.0). Samples were sonicated (VirTis VirSonic 100, SP Industries, Gardiner, NY) three times with each sample snap frozen in liquid nitrogen in-between each sonication. Samples were then centrifuged (10,000 × g) and the resulting supernatants were stored at -20°C. Samples were quantified using a Pierce BCA Protein assay kit (Thermo Scientific, Rockford, IL).

Total protein samples were separated by sodium dodecyl sulphate polyacrylamide gel electrophoresis (SDS-PAGE) containing 12% (w/v) acrylamide after being treated with 2% (w/v) β-mercaptoethanol, and heated at 80°C. The resulting gels were stained with Coomassie blue or transferred to a nitrocellulose membrane (Amersham Hybond-N, GE Healthcare, Buckinghamshire, UK) that was subsequently blocked in 5% (w/v) powdered milk solution. Blocked membranes were incubated with a primary AOX antibody (Agrisera AS06 152, Vännäs, Sweden) raised against *C. reinhardtii* AOX1 at a dilution of 1:2000, and a secondary Anti-rabbit IGg peroxidase antibody (Sigma A6154, St. Louis MO) was used at a dilution of 1:10,000. Membranes were washed between incubations with Tris Buffered Saline (TBS) with 0.1% Tween 20. Blotted membranes were visualized using a commercial ECL Detection kit (GE Healthcare Amersham ECL Western Blotting Detection Reagents, Buckinghamshire, UK) and exposed to film paper (Super RX, Fujifilm Corp., Tokyo).

2.6 Cellular respiration measurements

Whole cell rates of oxygen consumption were measured in the dark at 15ºC using an aqueous phase Clark type oxygen electrode (Hansatech Ltd., King's Lynn, UK). Measurements were carried out using cell cultures grown to mid-log phase in glass tubes submerged in temperature-controlled aquaria. Both UWO241 and 325R were grown in glass tubes aerated with filtered ambient air in order to maintain consistent growth conditions at optimal growth temperatures (10°C or 24°C) in order to prevent any growth condition variables from influencing respiration rates.

Before measurements were taken, cell cultures were concentrated via centrifugation and resuspended in HS medium supplemented with ammonium, nitrate, or ammonium plus 5 mM hydrogen peroxide. In the case of 325R cultures the HS medium did not contain 10 mM salt. After concentrating and shifting cells to new growth medium, cultures were allowed to recover for 12 hours before measurements were taken. Aliquots of cells (1.5 mL) were transferred from their growth environment into a water-cooled measurement chamber equipped with a magnetic stirrer.

The alternative and cytochrome pathway capacities were measured by using the inhibitors potassium cyanide (KCN) and salicylhdroxamic acid (SHAM), which block the flow of electrons through the cytochrome and alternative pathways, respectively (Molen et al. 2006). The alternative pathway capacity was calculated based on the rate of oxygen consumption in the presence of 1 mM KCN, while calculation of the cytochrome pathway capacity was the rate of oxygen consumption in the presence of 2 mM SHAM. The residual rate of oxygen consumption in the presence of both KCN and SHAM was subtracted from all measurements of total, AP, and CP respiration.

Stock solutions of KCN (1M) were prepared in sterile dH_2O, and stock solutions of SHAM (0.4 M) were prepared by dissolving in 100% ethanol. At least two biological replicates and at least three technical replicates were used to measure oxygen consumption levels in dark conditions, in the presence of KCN, in the presence of SHAM, and with both inhibitors present. Rates of photosynthetic oxygen evolution were observed initially before the

addition of any inhibitors by exposing samples to 200 µmol photons $m^{-2} s^{-1}$ of red wavelength light (centered at 650 nm) within the measurement chamber.

The rates of oxygen consumption were calculated relative to the total chlorophyll concentration of cell cultures through spectrophotometric analysis. To measure chlorophyll, aliquots of cell cultures were spun down at $16,100 \times g$ for five minutes and the resulting supernatant was removed by aspiration. Cell pellets were dissolved by mixing in 1.0 mL of 90% (v/v) acetone. These suspensions were centrifuged as before to pellet insoluble particles. The absorbance of the resulting supernatant was measured at 647 and 664 nm (Cary 50 Bio; Varian Inc., Palo Alto, CA, USA). At least 4 chlorophyll measurements were taken for each cell culture, and the concentrations of chlorophyll *a* and chlorophyll *b* were calculated using appropriate equations (Jeffery and Humphrey 1975). Chlorophyll samples were diluted during analysis to gather measurements within acceptable absorption values, and total calculated chlorophyll values were adjusted based on both the dilution factor, and the factor by which cells were concentrated through centrifugation when shifting cells to new growth medium.

3 Results

3.1 Isolation and sequence analysis of AOX cDNA and amino acid sequences

A cDNA library prepared from cells of UWO241 was used to isolate and amplify the *AOX1* gene. The library was prepared from cells grown at 10ºC in HS medium under constant light. Isolates of mRNA were cloned into a ZAP cDNA synthesis vector, which was then used to amplify *AOX1* from the cloned cDNA library.

Because there was no known sequence of *AOX1* from UWO241, an amplification strategy was developed that consisted of obtaining the entire sequence by amplifying two overlapping sections of the cDNA. For each PCR reaction, one primer was homologous to the known vector sequence while the second primer was designed based on a highly conserved region of the *AOX1* sequence for *C. reinhardtii*. The latter primer was designed based on conserved regions of the *C. reinhardtii AOX1* (XM_001694553) nucleotide sequence that translated into highly conserved motifs in the AOX1 amino acid sequence (XP_001694605.1). Amplification of *AOX1* sequence in this manner resulted in two fragments that were 981 and 859 bp after removal of vector-specific nucleotides (Figure 3-1).

Sequence analysis showed that the two amplicons had an overlapping sequence of 317 nucleotides, and a unique sequence of 1,522 bp cDNA (Appendix B). *In silico* translation of this 1,522 bp amplicon showed that the longest open reading frame sequence had a single open reading frame (ORF) encoding a 356 amino acid polypeptide (Figure 3-1A) with a calculated mass of 39.9 kDa. The ORF was flanked by 5' and 3' untranslated regions of 207 bp and 244 bp, respectively. The G + C content of the AOX1 sequence was 63.5%, which is similar to that of *C. reinhardtii AOX1* at 62.1%. Compared to most organisms this GC content would be considered high, although it seems to be typical of gene sequences for many photosynthetic algal species.
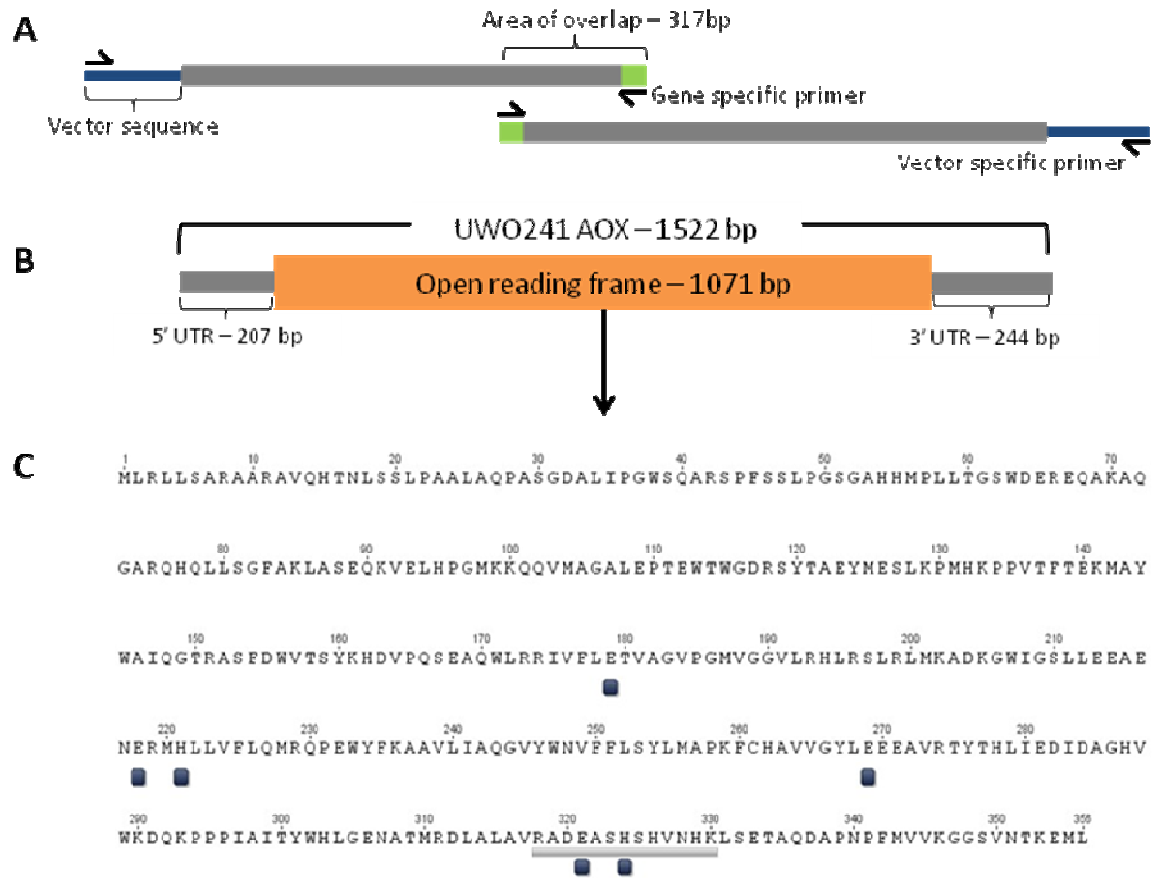
Figure 3- 1 Schematic representation of the isolation of AOX1 cDNA of *Chlamydomonas sp*. UWO241 from a cDNA library, and the deduced amino acid sequence of UWO241 AOX1.

Two gene-specific and two cDNA library vector-specific primers (small arrows) were used to generate two overlapping amplicons that span the entire cDNA insert (A). These two fragments were edited to remove the vector-specific sequence, and oriented using the overlapping sequence to produce a full length cDNA sequence (B). A single uninterrupted open reading frame was located and used to extrapolate an amino acid sequence. The deduced amino acid sequence (C) shows the conserved iron-binding residues (black squares) and the hypothesized AOX antibody binding epitope (grey bar).

The BLAST algorithm available at NCBI was used to determine similarity among the cloned 1522 bp cDNA and other sequences available in the GenBank databases.   The entire nucleotide sequence aligned with 73% identity to the *C. reinhardtii AOX1* gene when aligned using the NCBI Megablast nucleotide alignment tool with standard search parameters. The Megablast search was conducted using a search of the entire NCBI database as well as just the *C. reinhardtii* genome. In the case of the Megablast alignment with the *C. reinhardtii* genome, only one positive result aligning the UWO241 sequence to *C. reinhardtii AOX1* was returned. As previously noted, *C. reinhardtii* contains two *AOX* genes designated *AOX1* and *AOX2* (Dinant et al. 2001). Nucleotide alignment with the *C. reinhardtii AOX2* gene was possible considering the inherent similarities between *AOX1* and *AOX2* when using less stringent alignment parameters associated with the NCBI tblastn tool. Because of the high similarity of the total UWO241 *AOX* nucleotide sequence with *C. reinhardtii AOX1*, and the lack of high similarity with *C. reinhardtii AOX2*, the gene isolated from the UWO241 cDNA library was designated *AOX1*.

The deduced 356 amino acid UWO241 AOX1 protein was similar in length to that of *C. reinhardtii* AOX1, which is composed of 360 residues. The proportions of amino acids that make up the UWO241 AOX1 compared to that of *C. reinhardtii* were of particular interest since UWO241 AOX1 had lower amounts of proline (5.6% vs. 8.3%), and alanine (11.5% vs. 15.6%), but higher amounts of lysine (5.1% vs. 2.2%) and tryptophan (3.4% vs. 1.1%).

Figure 3-2 shows the results of aligning the deduced AOX1 protein sequence from the UWO241 *AOX1* cDNA sequence with AOX protein sequences of six other species. The deduced UWO241 AOX1 amino acid sequence aligned with known conserved regions to reveal residues related to iron-binding ligands (Figure 3-2). The UWO241 *AOX1* contained the four glutamic acids (Glu179, Glu218, Glu269, and Glu321) and two histidines (His221, and His 324) in conserved motifs that facilitate iron atom binding (Figure 3-1C and Figure 3-2). The UWO241 AOX1 sequence did not contain the conserved cysteine residue associated with angiosperm dimerization. In plant species, the dimeric form of
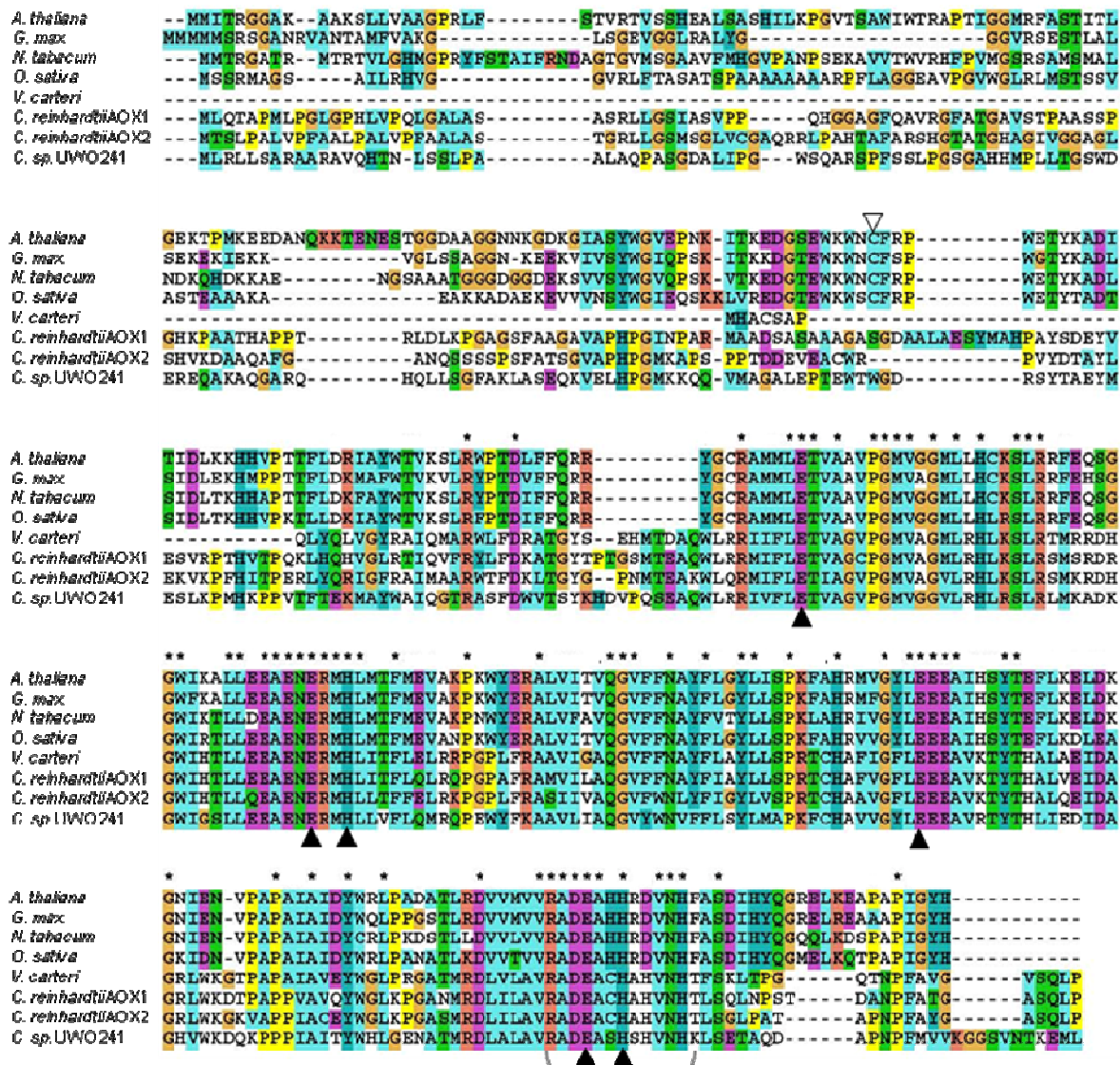
Figure 3- 2 Amino acid sequence alignment of eight AOX proteins.

Asterisks above residues indicate amino acids that are conserved in all sequences. Conserved iron-binding residues are indicated by black arrows. The conserved cysteine residue indicated by the white arrow is the hypothesized locus for dimerization in angiosperm AOX proteins. The grey bracket indicates the hypothesized AOX antibody epitope. The alignment was completed using the Clustal X software with its standard colouring scheme denoting alignment scores. Protein accession numbers and full species names are listed in the 'Materials and Methods'.

AOX is thought to have low activity, while the monomeric form has a higher activity. This has been suggested as a method for regulating the activity of AOX in plants (Umbach and Siedow 1993).

Through the use of the NCBI blastp alignment tool the deduced UWO241 AOX1 protein sequence was aligned to show identical and positive residue similarities with six species. The alignment of UWO241 AOX1 with the *C. reinhardtii* AOX1 showed 57-73% identity (over 226 residues), and aligned with the C. reinhardtii AOX2 with 48-65% identity (over 304 residues). The UWO241 AOX1 had greater homology when aligned with *C. reinhardtii* and the multicellular chlorophyte *Volvox carteri* (60-74% over 203 residues). Lower levels of similarity were observed when compared to the plant species *A. thaliana* (43-61% over 242 residues), *G. max* (40-58% over 277 residues), *O. sativa* (47-62% over 230 residues), and *N. tabacum* (41-59% over 242 residues).

3.2 Immunoblotting of AOX protein in mesophile and psychrophile

In addition to cloning the UWO241 *AOX1* sequence, another major aim of the thesis was to identify the presence of the AOX protein through the use of standard immunological protocols. A polyclonal antibody raised against AOX from *C. reinhardtii* was available. This antibody has been used previously and cross-reacts with a protein that migrates to a size of approximately 38 kDa (Pakkiriswami et al. 2009)

As shown in Figure 3-3, western blotting using the *C. reinhardtii* polyclonal antibody for AOX produced no cross-reactivity in UWO241 total protein isolations. In *C. reinhardtii* 325R the antibody produced a strong ≈38 kDa signal with a minor secondary signal just below the 35 kDa mark. The western blot for UWO241 produced no signal around the predicted molecular mass of 39.9 kDa.

The lack of cross-reactivity could be due to a technical issue related to the initial isolation technique. However, attempts to identify the factors preventing cross-reactivity were investigated through the use of different protein isolation techniques, multiple blot
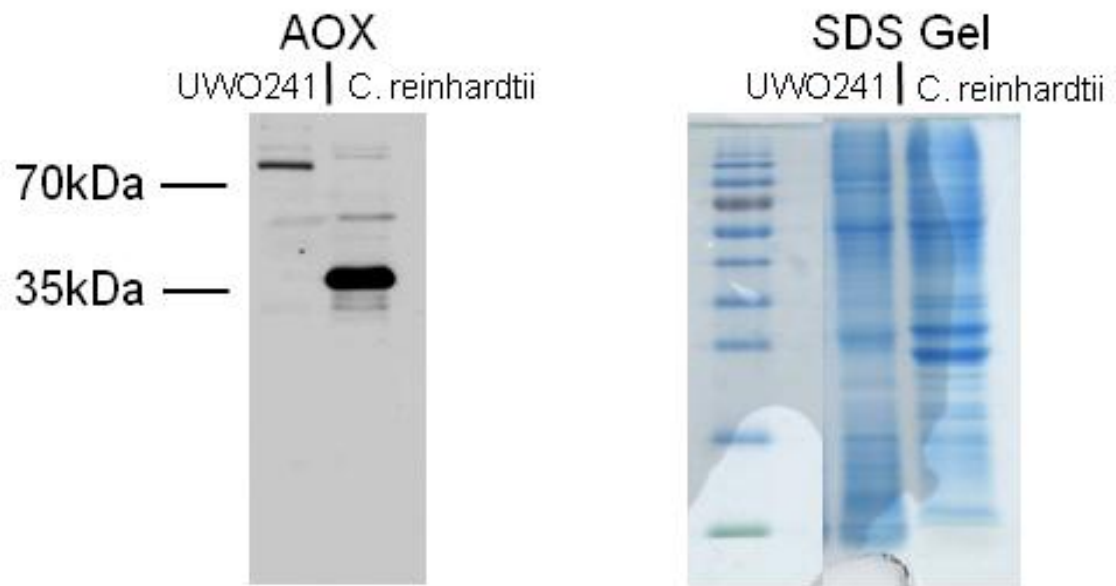
Figure 3- 3 Immunoblot with AOX antibody raised in *C. reinhardtii* shows no cross reactivity in total protein samples from the psychrophile *Chlamydomonas sp.* UWO241 (left figure labeled 'AOX').

Both UWO241 and *C. reinhardtii* 325R cells were grown in nitrate growth medium and total protein was separated via SDS-PAGE (right figure labeled 'SDS Gel'). Resulting gels were stained with coomassie blue to show protein migration (stained protein standard ladder shown indicating molecular mass in kDa).

rinsing techniques, and different ratios of primary and secondary antibodies (data not shown). This lack of cross-reactivity occurred despite what appears to be adequate migration of polypeptides through SDS-PAGE as is evident in coomassie blue stained gels (Figure 3-3). High molecular mass banding patterns in western blots were observed in both species and may indicate non-specific antibody binding.

3.3 Changes in AOX transcript abundance under nitrate and hydrogen peroxide stress

In *C. reinhardtii, AOX1* transcript abundance increases strongly in response to changes to the growth environment. Two changes in particular are a shift in nitrogen source from ammonium to nitrate (Pakkiriswami et al. 2009) and treatment of cells with hydrogen peroxide (Molen et al. 2006), both of which promote accumulation of *AOX* transcripts. To investigate the biological function of AOX in UWO241, three stresses were used in order to examine the cellular response by measuring *AOX* transcription accumulation. Under ammonium growth conditions *C. reinhardtii* to shows no accumulation of *AOX*; however, accumulation of *AOX* transcript in response to nitrate is a very rapid reaction having been shown to occur within 0.5 hours of exposure (Molen et al. 2006).

To assess changes in transcript abundance, RNA was isolated from cells as a function of time after shifting the growth medium of cell cultures from high salt medium (HS)-NH_4 to HS-NO_3, or the addition of 5 mM hydrogen peroxide to HS-NH_4. The semi-quantitative RT-PCR (sqRT-PCR) results for *C. reinhardtii* 325R showed that under ammonium growth conditions there was very little baseline expression of *AOX* (Figure 3-4B). Within the first 0.5 hours of shifting 325R cultures from ammonium to nitrate medium, the amount of *AOX* transcript rose to approximately 50 × the amount of relative transcript abundance observed in cells grown in ammonium (Figure 3-4B). The amount of transcript accumulation continued to rise to approximately 73 × the amount of relative transcript abundance at the four hour time point. At six hours the amount of *AOX* transcript fell below the increased levels observed at 0.5 hours but still represented a 37-fold increase in transcript abundance.

Figure 3- 4 Relative transcript abundance of *AOX* in *Chlamydomonas sp*. UWO241 (A) and *C. reinhardtii* 325R (B) as a function of time following a shift in nitrogen source from ammonium to nitrate containing media.

Values are based on adjusted volume analysis of imaged gels and calculated based on the ratio of loading control to *AOX* signal. Ribosomal loading control and *AOX* banding patterns of typical gels are inset. Values represent at least three technical replicates and standard error bars are shown.

Under ammonium growth conditions UWO241 showed a high amount of *AOX* transcript abundance compared to *C. reinhardtii* (Figure 3-4A and B). Once placed under nitrate growth conditions, there was no immediate rise in *AOX* transcription, and the change in transcription was comparatively smaller than in the mesophile. Transcript abundance increased for the first hour and after six hours of exposure to nitrate was approximately 0.35 × the relative transcript abundance observed at time zero.

Similar to the response of *AOX* transcription abundance after a change in nitrogen source, hydrogen peroxide has been used to produce a change in *AOX* transcription accumulation (Molen et al. 2006). One of the current hypotheses explaining the biological function of AOX is that it mitigates the accumulation of reactive oxygen species within the mitochondria. To examine this, cells were grown under optimal temperatures with ammonium growth medium and 5 mM hydrogen peroxide was added once cells reached the mid-log growth phase.

A rapid accumulation of *AOX* transcript was observed in *C. reinhardtii* 325R after the addition of hydrogen peroxide. After 0.5 hours of exposure, transcript levels increased to approximately 150 × the relative abundance observed under ammonium (Figure 3-5B). After four hours of exposure, the amount of *AOX* transcript fell to levels observed under ammonium growth conditions.

The reaction observed upon exposure of UWO241 to hydrogen peroxide was different compared to *C. reinhardtii*, whereby the amount of *AOX* transcript reduced immediately after exposure (Figure 3-5A). A high amount of *AOX* transcript under ammonium conditions was observed at time zero. The amount of *AOX* transcript abundance after the first 0.5 hours reduced rapidly to 0.156 × the relative transcript abundance measured at time zero. The amount of *AOX* transcript remained at low levels throughout the six hour exposure but remained consistent at approximately 0.159 × the relative transcript abundance measured at time zero.
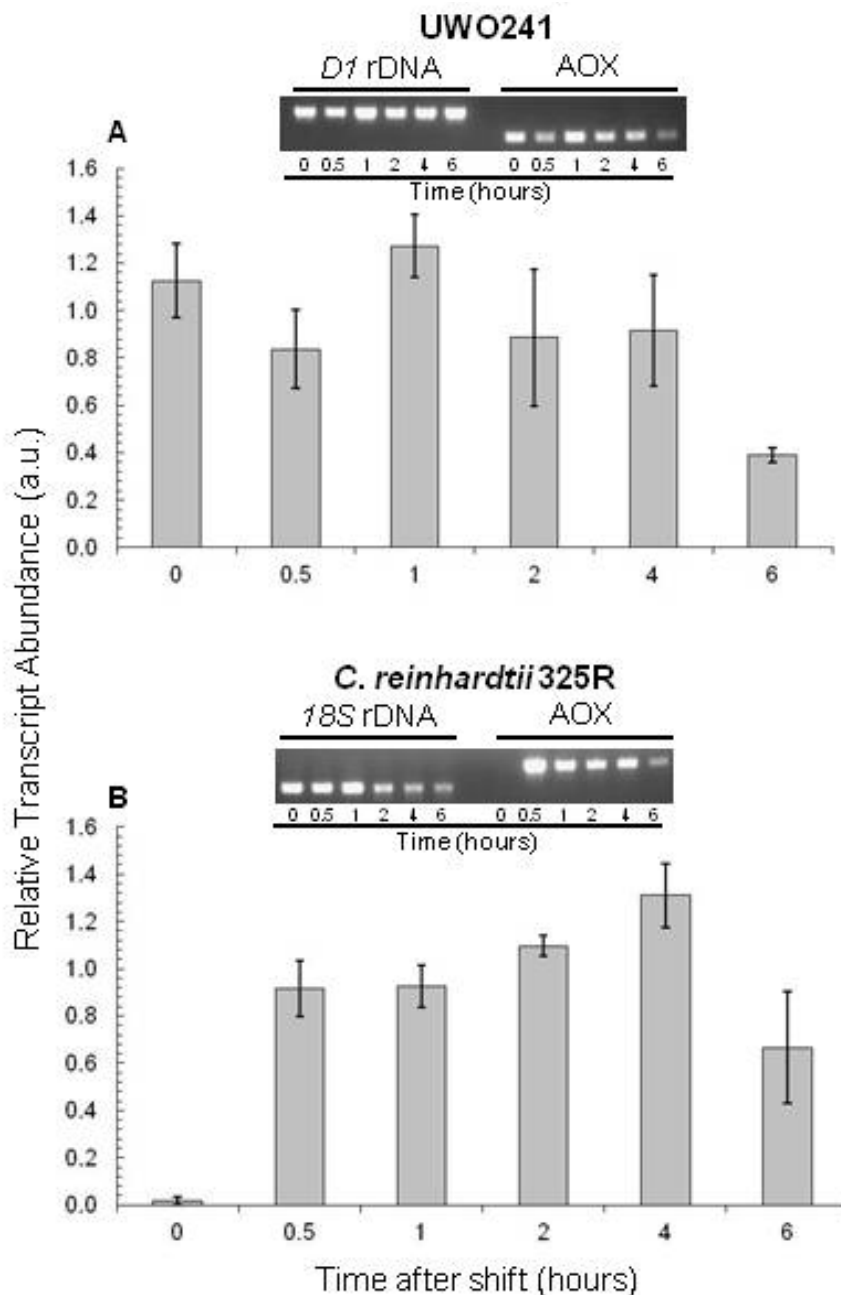
Figure 3- 5 Relative transcript abundance of *AOX* in *Chlamydomonas sp.* UWO241 (A) and *C. reinhardtii* 325R (B) as a function of time following the addition of hydrogen peroxide.

Values are based on adjusted volume analysis of imaged gels and calculated based on the ratio of loading control to *AOX* signal. Ribosomal loading control and *AOX* banding patterns of typical gels are inset. Values represent at least three technical replicates and standard error bars are shown.

3.4 Changes in *AOX* transcript abundance under heat stress

As shown by Possmayer et al. (2011), a number of genes in UWO241 are induced upon heat stress including: *LHCBM7*, *FED-1, HSP90A*, *HSP90C*, and *HSP22A*. These inductions were measured after shifting UWO241 cultures from 10°C to 24°C over a 12 hour period. In the present study the abundance of *AOX1* transcript in UWO241 was investigated under the same temperature and nutrient treatments for 48 hours. This was done in concert with an equivalent heat stress treatment in *C. reinhardtii* where cultures were shifted from 28ºC to 40ºC.

Figure 3-6 shows the *AOX* transcript abundance for both *C. reinhardtii* 325R and UWO241 upon heat stress. In *C. reinhardtii*, after three hours the amount of *AOX* transcript rose nearly eight-fold, and continued to rise to 29.3x the time zero abundance after 48 hours of heat stress (Figure 3-6B). As in the nitrate and hydrogen peroxide results, the abundance of *AOX* transcript was very low at time zero under optimal temperature and ammonium growth conditions (See Figures 3-4B, 3-5B, and 3-6B).

The psychrophile's response to being shifted from 10ºC to 24ºC under ammonium growth conditions showed an approximately 54% decrease in *AOX* transcript levels as early as three hours after the initial stress (Figure 3-A). Transcript levels remained below the initial level up to 24 hours after the stress. Measurements of *AOX* transcript abundance 48 hours after the initial heat stress showed an approximately 65% increase in *AOX* transcript abundance from 24 to 48 hours. This was despite the consistent transcript levels of rDNA loading control (D1 rDNA).

3.5 Total, alternative pathway, and cytochrome pathway respiration capacities

Gas exchange using intact UWO241 cells was measured at 15°C using a Clark-type oxygen electrode. Rates of oxygen consumption under dark conditions were used to measure total mitochondrial respiration, and the addition of KCN and SHAM were used
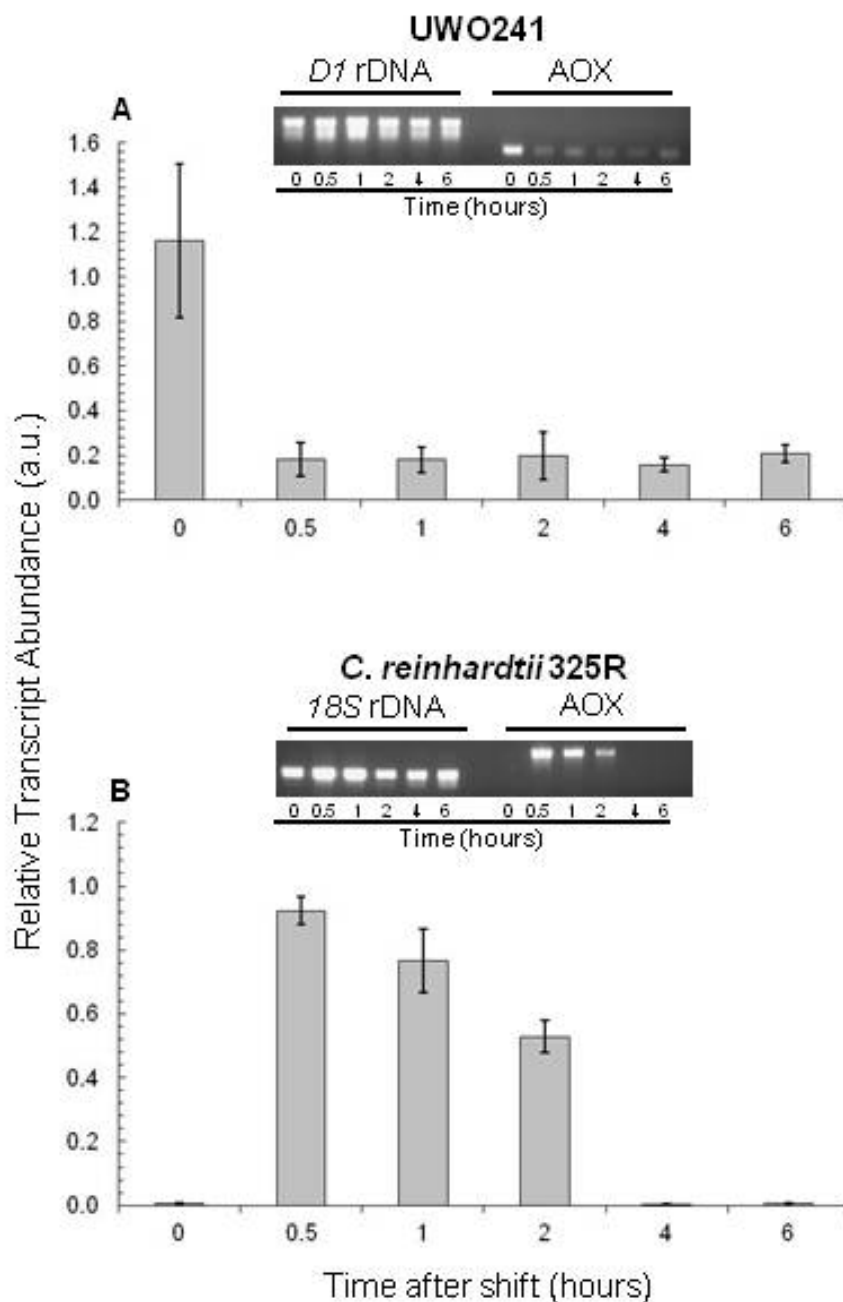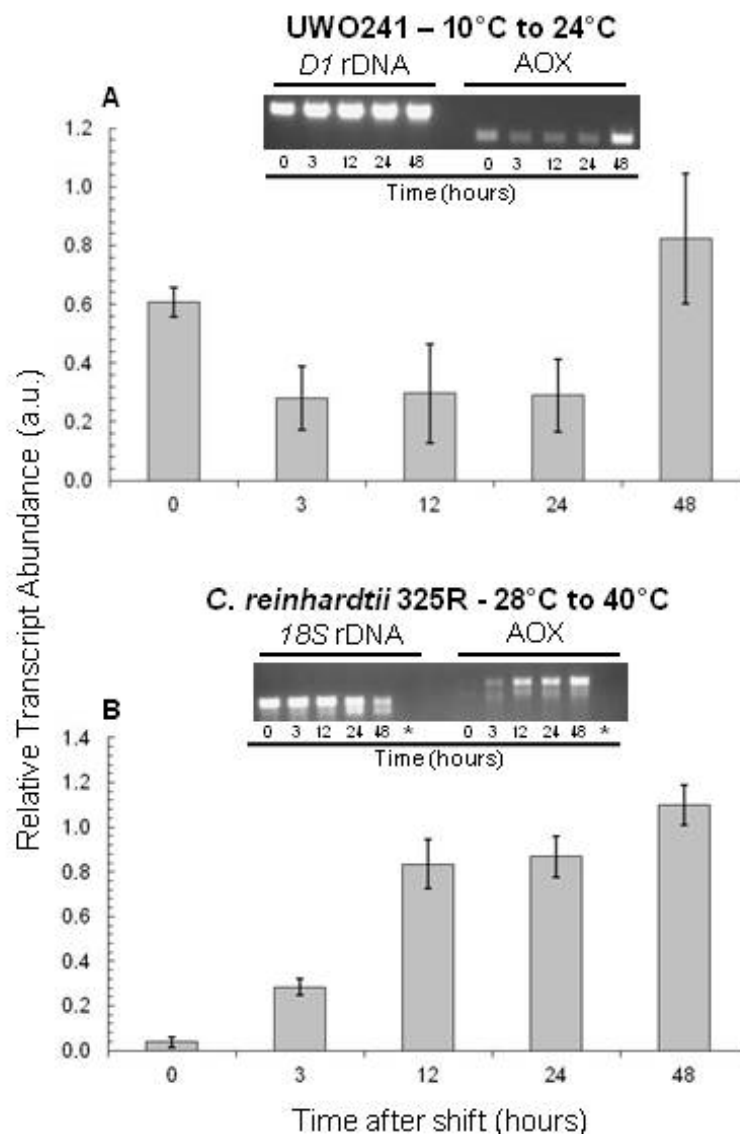
Figure 3- 6 Relative transcript abundance of *AOX* in *Chlamydomonas sp.* UWO241 (A) and *C. reinhardtii* 325R (B) upon heat stress treatment.

Cells were grown in ammonium growth medium at optimal temperatures, represented by time point zero. Heat stress conditions for UWO241 were created by shifting cells from 10ºC to 24ºC while *C. reinhardtii* 325R was shifted from 28ºC to 40ºC. Values are based on adjusted volume analysis of imaged gels and calculated based on the ratio of loading control to *AOX* signal. Ribosomal loading control and *AOX* banding patterns of typical gels are inset. Asterisks (gel image in B) show typical negative control lanes that underwent RT-PCR without RNA polymerase. Values represent at least three technical replicates and standard error bars are shown.

to inhibit CP and AP respiration, respectively (Figure 3-7). The rates of oxygen evolution due to photosynthetic electron transport, and oxygen consumption due to mitochondrial respiration have been measured previously in UWO241 (Possmayer et al. 2011). These measurements were conducted under optimal and supraoptimal temperature conditions in ammonium growth medium. Considering the *AOX* transcript abundance under ammonium growth conditions observed here, and the concurrent reduction of *AOX* transcript under nitrate and hydrogen peroxide conditions, the mitochondrial function of UWO241 was investigated. The concept that mitochondrial enzyme activity is tied to temperature was also investigated. *C. reinhardtii* cultures were used to measure oxygen consumption under ammonium and nitrate conditions at 15°C and compared to total respiration of UWO241 at the same temperature. Measurements were taken at 15°C because this temperature lies outside the optimal growth rate temperature of both species, yet appreciable rates of respiration can still be observed.

The observed decrease in total respiration from ammonium to nitrate, or hydrogen peroxide was 20.5 and 54.5%, respectively (Figure 3-8). Under ammonium growth conditions the measured AP capacity was 29.1% higher than the CP capacity. The observed AP and CP capacities under nitrate and hydrogen peroxide growth conditions were almost equivalent to the total respiration values observed. The ability of whole cell cultures to undergo mitochondrial respiration in the presence of KCN or SHAM indicates that total respiration values are indicative of the apparent ability of UWO241 to rely solely on AP capacity or CP capacity, respectively.

Total mitochondrial respiration was measured in the *C. reinhardtii* 325R in order to examine the ability of non-cold-adapted mitochondrial respiration to function at a cold temperature. After twelve hours of incubation at an optimal growth temperature of 24°C under ammonium and nitrate conditions, total mitochondrial respiration was measured at 15°C. Total respiration in *C. reinhardtii* under ammonium and nitrate conditions was measured to be 90.0 and 84.4% less than the total respiration measured in UWO241 under the same conditions (Figure 3-9).
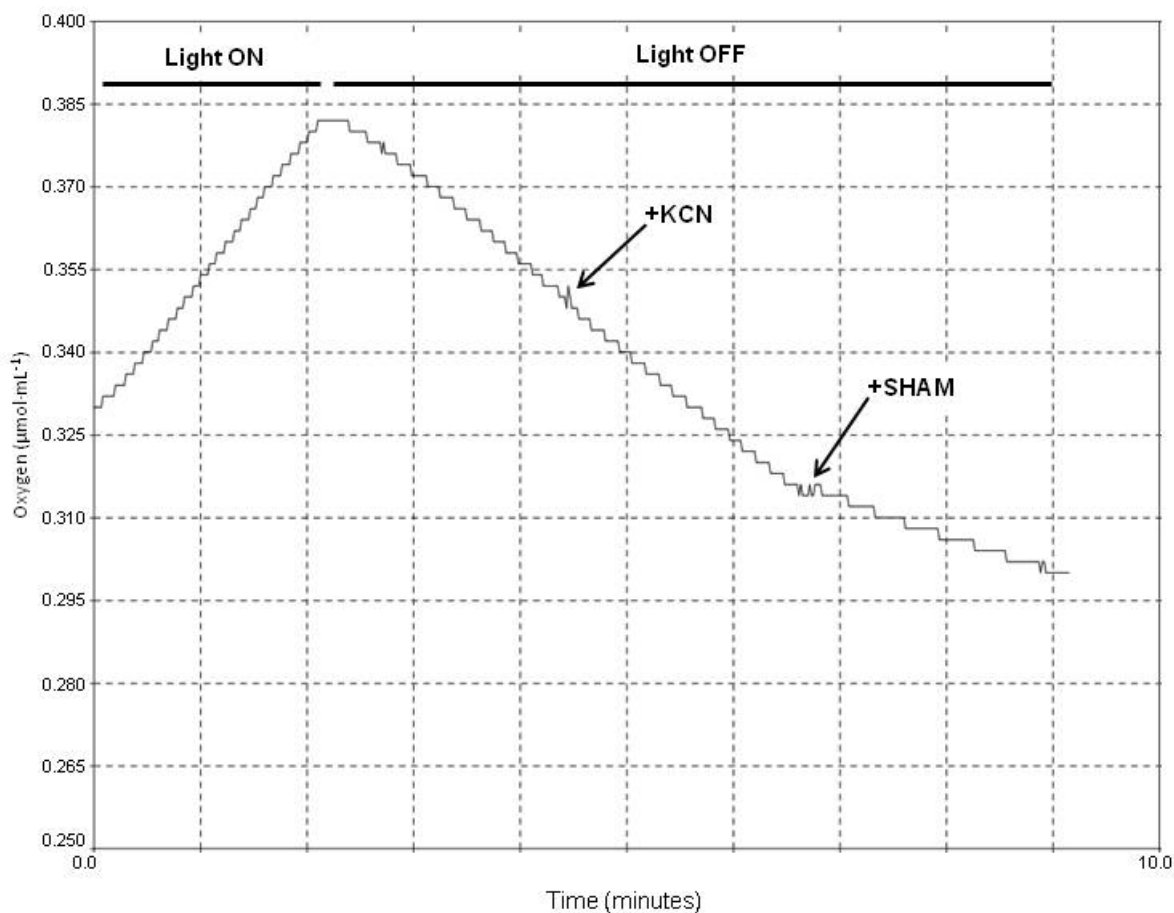
Figure 3- 7 Representative trace of whole cell oxygen measurements of *Chlamydomonas sp*. UWO241 taken at 15°C under ammonium growth conditions.

Aliquots of cell cultures (1.5 mL) were placed in a closed measurement chamber and exposed to red light (650 nm). Under dark conditions, cells undergo mitochondrial respiration until the cytochrome pathway inhibitor potassium cyanide (KCN) is added. Residual non-mitochondrial oxygen consumption is measured after addition of the alternative pathway inhibitor salicylhydroxamic acid (KCN + SHAM) to block both electron transport pathways in the mitochondria.
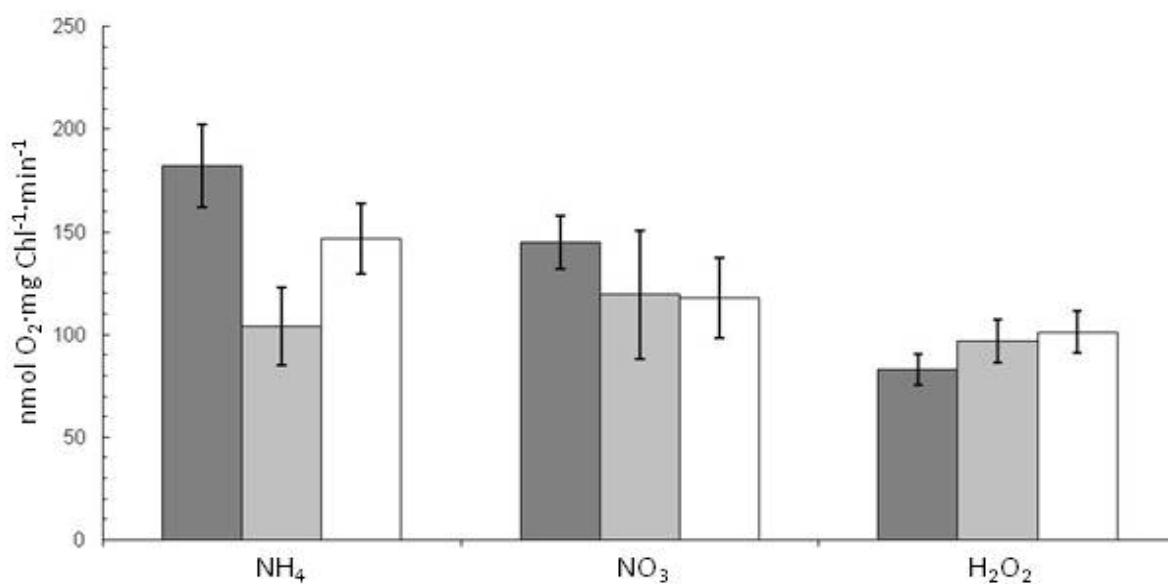
Figure 3- 8 Respiration measurements in *Chlamydomonas sp*. UWO241 after a 12 hour incubation in ammonium, nitrate, and ammonium + 5 mM hydrogen peroxide growth mediums.

Oxygen consumption rates were used to measure total respiration (dark grey bars), cytochrome pathway (light grey bars), and alternative pathway (white bars) capacities at 15ºC. Values represent at least two biological replicates and at least three technical replicates for each measurement. Standard error values are shown.
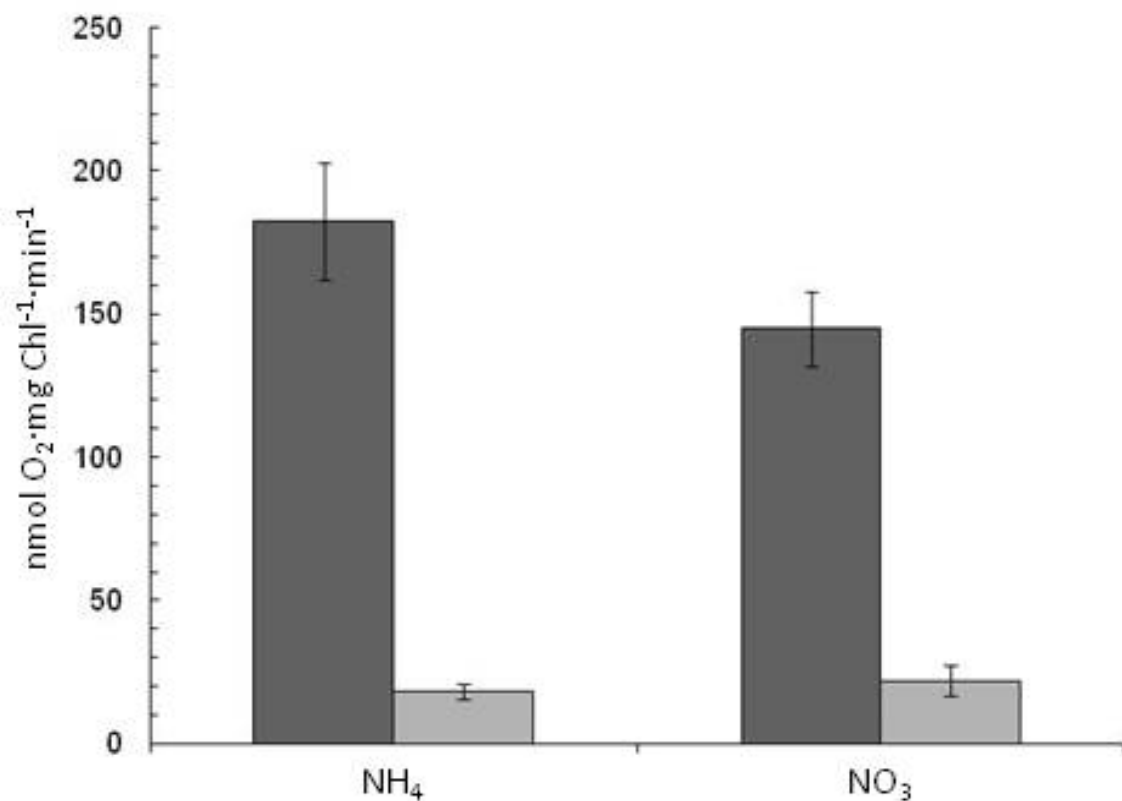
Figure 3- 9 Total respiration measurements in *C. reinhardtii* 325R (light bars) and the psychrophilic *Chlamydomonas sp*. UWO241 (dark bars) under ammonium and nitrate growth conditions.

Cultures of UWO241 and 325R were grown at optimal growth temperatures of 10ºC and 24ºC, respectively, before measurements were taken at 15ºC. Values represent at least two biological replicates and at least three technical replicates. Standard error bars are shown.

4   Discussion

It has been estimated that the lakes of the McMurdo Dry Valley, including Lake Bonney, have been isolated from the Antarctic Ocean for approximately 2,000 to 15,000 years (Priscu 1997). As well, vertical mixing times in the lakes of the McMurdo Dry Valley are also thought to occur on the order of tens of thousands of years due to the permanent layer of thick ice (3 to 5 m) (Priscu 1997). The Antarctic lake environment from which *Chlamydomonas sp.* UWO241 was isolated is in stark contrast to the temperate soil environments where *Chlamydomonas reinhardtii* is found (Harris 1989). The geographic isolation of UWO241 to Antarctica and the disparate habitats of these two green alga likely trigger adaptive differences in both the structure of AOX and its regulation.

Upon examination of the deduced primary amino acid sequence of *AOX1* from UWO241, two main differences suggest cold-adaptation when compared to the AOX1 of *C. reinhardtii*. First, there is a lower proportion of proline residues in UWO241 AOX. Lower proportion of proline is seen consistently in enzymes isolated from psychrophilic enzymes compared to their mesophilic homologues. For example, a decrease in proline residues within the α-helices of psychrophilic enzymes has been observed in the citrate synthase of Antarctic bacteria (Russel et al. 1998) and the Rubisco of Antarctic *Chloromonas* (Devos et al. 1998). Since the side-chain of proline is cyclic it does not readily form hydrogen bonds and is therefore thought to interfere with hydrogen bonding in secondary structures. This observation has been linked to the conformational flexibility associated with cold-adaptation since a reduction of hydrogen bonding in α-helices by increased proline would contribute to the overall flexibility of a cold-adapted enzyme (Russell et al. 1998).

Second, lower proportions of alanine and higher proportions of lysine and tryptophan were observed in the AOX1 sequence from UWO241 as compared to *C. reinhardtii*. The replacement of amino acids having small aliphatic side-chains (e.g. alanine) with those containing bulkier aromatic side-chains (e.g. lysine and tryptophan) has been suggested to create less conformationally stable proteins. This concept of conformationally flexible proteins is widely accepted to be a ubiquitous characteristic of cold-adaptation within primary amino acid structures (Zecchinon et al. 2001). To be catalytically active at low

temperatures, cold-adapted enzymes require more flexible structures (Siddiqui and Cavicchioli 2006). This also helps explain the death of psychrophiles at higher temperatures since an increase in conformational flexibility bears the consequence of denaturation at temperatures above 20ºC.

The biochemistry of the reaction catalyzed by AOX has been well characterized, as has the protein structure of AOX. AOX facilitates the oxidation of ubiquinol in order to catalyze the reduction of oxygen to water (Berthold et al. 2000). This reaction requires a diferric core to bind oxygen. The conserved Glu and His iron-binding residues are localized to highly conserved motifs in many species (McDonald 2009). Research into the deduced secondary and tertiary structure of AOX has also revealed a conserved 3D conformation that suggests an interfacial orientation in the inner mitochondrial membrane (Albury 2009). However, a clear biological function for AOX is well established only for thermogenic species of plants in the family Araceae (Meeuse 1975).

In *C. reinhardtii, AOX* is strongly upregulated in response to nitrate. Several studies have shown a strong induction of *AOX* in *C. reinhardtii* under nitrate conditions, and repression in the presence of ammonium (this study; Quesada et al. 1998; Pakkiriswami et al. 2009; Molen et al. 2006). This coordinated expression seems to be associated with the location of the *AOX* gene within one of the nitrate assimilation related (NAR) gene clusters (Quesada et al. 1998).

A potential reason for why *AOX* is induced by nitrate is that nitrate must be enzymatically reduced to produce ammonium which is energetically costly (Fernandez and Galvan 2008). However, the role for increased alternative pathway (AP) respiration and ATP production under nitrate conditions is still not understood. The divergence of *C. reinhardtii* and UWO241 is clearly observed here since the coordinated expression of *AOX* in response to nitrate does not seem to occur in the psychrophile.

One of the surprising findings shown here is that the strong induction of *AOX* upon shifting cells from ammonium to nitrate containing media in *C. reinhardtii* was not observed in UWO241. In fact, the opposite appears to be true; UWO241 shows constitutively higher

basal levels of *AOX* transcript under optimal temperature and ammonium growth conditions that seem unaffected by a shift to nitrate.

One could argue that the lack of induction of *AOX1* in UWO241 in response to a shift from ammonium to nitrate may simply be due to the slow kinetics of the response. The experiment with *C reinhardtii* was conducted at 28ºC while the nitrogen shift experiment for UWO241 was conducted at 10ºC.

Most biological processes have a Q_{10} of approximately 2. This means the rate of a reaction doubles for each 10ºC increase in temperature (Feller and Gerday 2003). Since the rapid increase in *AOX* transcript abundance at 28°C in *C. reinhardtii* occurred over a period of 0.5 hours, even with a Q_{10} value of 6, implying the same reaction at 10°C would take three hours in UWO241, the amount of *AOX1* transcript in UWO241 shows little change even after six hours of exposure. This suggests that the wide range of time points included in my kinetic analysis of transcript abundance was more than enough to account for any reasonable delay in transcription brought about by the temperature differences. This suggests an alternative mode of *AOX* regulation in UWO241, a hypothesis that could be tested in the future by examining the loci of *AOX1* and potential regulatory elements in relation to the *NAR* gene cluster within the genome of UWO241.

The strong upregulation of *AOX1* in *C. reinhardtii* in response to nitrogen assimilation may be a product of its adaptation to a soil environment (Fernandez and Galvan 2008). Abiotic and human activities can cause rapid fluctuations in the availability of nutrients in different soil ecologies (Tubea et al. 1981). This is in stark contrast to the highly stable conditions found in Lake Bonney, Antarctica. The extremely slow rate of vertical mixing has created a stable gradient of nitrogen sources, oxygen, and salt (Priscu 1997). In addition to the observed stability in nutrients, the amount of photosynthetically active radiation (PAR) available 17 m below the surface ice is consistently low. Measurements throughout the Antarctic seasons show a range of PAR between 14 and 23 µmol photons·m^{-2}·s^{-1}, and a nearly total absence of PAR during the Antarctic winter (Lizotte and Priscu 1994). This dichotomy in ecological niches is the context upon which the divergence of these two algal species is based, and may contribute to the biological function of AOX in UWO241.

Another intriguing observation made here is the rapid decline in *AOX* transcript abundance upon exposure to hydrogen peroxide. Many species have shown increases in *AOX* transcription and protein accumulation upon exposure to hydrogen peroxide. *N. tabacum* (Maxwell et al. 1999), *Arabidopsis* (Sweetlove et al. 2002), and *C. reinhardtii* (Molen et al. 2006) all show induction of *AOX* in response to treatments that elicit oxidative stress. This has led to the suggestion that AOX is susceptible and responsive to increased levels of oxidants within the cell.

A decline in *AOX* transcript abundance upon direct exposure of UWO241 to hydrogen peroxide could most easily be explained by the fact that at the sub-lethal concentration used here global damage to nucleic acids and proteins by hydrogen peroxide prevent the accumulation of transcript. However, this seems unlikely considering the constitutive amounts of ribosomal (*D1* rDNA) transcript observed throughout the six hour period. A slight reduction in AOX protein accumulation in hydrogen peroxide-treated *Arabidopsis* mitochondria has been observed previously, which may be caused by cellular regulation or simply the damaging effects of hydrogen peroxide (Sweetlove et al. 2002). In fact, broad changes to protein accumulation have been observed in hydrogen peroxide-treated rice seedlings (Wan and Liu 2008). However to the best of my knowledge, an example of decreased *AOX* transcript abundance in response to hydrogen peroxide has not been reported in current literature.

The response of UWO241 to heat stress may also suggest a regulation of *AOX* distinct from that of *C. reinhardtii*. The transcript abundance of *AOX1* from UWO241 initially decreases upon exposure to a supraoptimal temperature, and then peaks at 48 hours after treatment. The higher accumulation of *AOX* transcript at 48 hours may represent a heat stress response characterized by an increase in heat shock proteins (HSPs) that has previously been observed in UWO241 (Possmayer et al. 2011) along with examples from psychrophilic yeast (Deegenaaars and Watson 1998), psychrophilic seaweed (Vayda and Yuan 1994), and *C. reinhardtii* (Gromoff et al. 1989) to name a few. In fact, Graf and Jakob (2002) have suggested that the induction of a heat stress response can elicit a concomitant induction of genes related to mitigation of ROS formation.

In addition, Possmayer et al. (2011) have suggested that UWO241 may undergo a programmed cell death (PCD) response when placed under prolonged heat stress. The expression of *AOX* as a deterrent to PCD has been hypothesized by Kern et al. (2007) and may be related to the increase in *AOX* transcript under heat stress observed here. However, it is of interest that the initial reaction of UWO241 to heat was a reduction of available *AOX* transcript after three and 12 hours. Again, this may simply be due to the damaging effect of the treatment as mentioned above; however, this does not appear to be the case since the abundance of loading control transcript is unaffected.

The post-translational modification by glutathionylation of psychrophilic enzymes has been shown to reduce the enzymatic degradation of a superoxide dismutase in *Pseudoalteromonas haloplanktis* (Castellano et al. 2008). Although this concept was not tested here, it may explain the apparent reduction in *AOX* transcript observed. Further study of this hypothesis would require measurement of AOX protein abundance to determine any modifications to the rate of AOX protein turnover.

One of the more frustrating aspects of this study was that attempts to measure the amount of AOX protein accumulation in UWO241 with a polyclonal antibody raised against *C. reinhardtii* were unsuccessful. Although the general location of the AOX antibody epitope is known (Finnegan et al. 1999), it would appear that the cold-adaptation of UWO241 has resulted in a significant alteration to the primary amino acid sequence and secondary structure of AOX within the conserved diiron binding motif that is thought to contain the site of antibody recognition.

The AOX antibody recognition site in *S. guttatum* was localized to the C-terminus by Finnegan et al. (1999). In support of this finding, a recent *in silico* analysis by McDonald (2009) aligned 19 AOX sequences in order to generate a consensus sequence that might predict the ability of an AOX antibody to cross-react at the proposed C-terminal epitope. The sequence predicted to allow for AOX antibody cross-reactivity reads: Arg-[Ala/Gln]-Asp-Glu-[Ala/Ser]-[His/Cys/Asp/Glu/Lys/Val]-His-[Arg/Ala]-[Asp/Glu/His/Leu/Val/Gly]-Val-Asn-His. The deduced amino acid sequence of UWO241 AOX1 shows two important differences within this predicted epitope. The sequence of UWO241 reads: Arg-Ala-Asp-Glu-Ala-Ser-His-Ser-His-Val-Asn-His. The sixth and eighth serine residues in the AOX

antibody epitope of UWO241 may create an area of higher polarity that does not allow for cross-reactivity. Structural differences like these must be ubiquitous in UWO241 since many antibodies for conserved polypeptides do not cross-react.

This has been examined by Szyszka and Hüner (personal comm.) who have reported unsuccessful attempts with several polyclonal antibodies raised against thylakoid membrane proteins LHCB1, Ferredoxin, and NDH-H, despite modifications to protein isolation and blotting techniques. Even a polyclonal antibody raised against *C. reinhardtii* for the widely conserved cytochrome oxidase (COX) does not cross-react in UWO241 total protein isolates (Appendix C).

Clearly, the deduced primary structure of AOX from UWO241 shows distinct differences when compared to *C. reinhardtii*. It therefore seemed prudent to examine the ability of UWO241 to undergo alternative pathway (AP) respiration after a shift in nitrogen source from ammonium to nitrate, or the addition of hydrogen peroxide. The data presented here suggest that UWO241 has a high AP capacity that is equal to or greater than the capacity for cytochrome pathway (CP) respiration, a result that is consistent with previous measurements in UWO241 (Possmayer et al. 2011). The capacity of the AP or CP refers to the ability of these pathways to be reduced due to a greater abundance of enzyme and reductants that can be observed as a greater rate of reaction. Considering the constitutive amount of *AOX* transcript under ammonium and nitrate conditions, it is not surprising that high basal AP respiration was observed. The observed loss of total, AP and CP respiration under hydrogen peroxide treatment is also not surprising considering the damaging effects of hydrogen peroxide to total respiration observed in previous studies (Maxwell et al. 2002; Molen et al. 2006).

As mentioned above, the ecological niches from which *C. reinhardtii* and UWO241 were isolated are very different. The stable environmental conditions of Lake Bonney were not simulated in this study since the optimal growth rate for UWO241 was observed at 10ºC under continuous 120 μmol photons$\cdot$m$^{-2}\cdot$s^{-1} light conditions in HS-NH$_4$ growth medium (Morgan-Kiss et al. 2006).   The light conditions used in the laboratory represent nearly 10 times the available light experienced by UWO241 in its Antarctic habitat (Lizotte and Priscu 1994). Previous work in *Arabidopsis* has shown that exposure to high light conditions can

cause an increase in *AOX* transcript and protein accumulation (Yoshida et al. 2007). This is in agreement with the hypothesis that an imbalance in electron transport within the chloroplast caused by excess light energy can be sensed by the mitochondria in order to elicit a change in the energy source or sink capacity of a photosynthetic organism (Wilson et al. 2006). The implications of these findings suggest that the regulation of mitochondrial respiration, including the AP, may be related to sensing imbalances in energy capture by photosynthetic electron transport.

This may be particularly important in UWO241 since it has existed under very low light conditions and permanent ice-cover for at least 200 years (Morgan-Kiss et al. 2006). Its adaptation to this cold, low-light environment may have included an ability to coordinate expression of *AOX* in response to a change in photosynthetic capacity. In fact, Szyszka et al. (2007) have shown that, in response to high-light treatment, UWO241 shows an increase in accumulation of phosphorylated polypeptides as well as little change in accumulation of light-harvesting polypeptides. This demonstrates a decreased sensitivity of UWO241 to high irradiance since the photochemical reduction of light harvesting polypeptides is not observed. This observation highlights the ability of UWO241 to respond to high-light conditions.

The explanation for this observation in UWO241 may lie in the dissipation of excess light energy through typical photochemical energy quenching responses such as non-photochemical quenching through the epoxidation of the xanthophyll cycle pigments (Szyszka et al. 2007). Another possible mode of energy dissipation beyond typical redistribution of light energy throughout the photosynthetic pigments and polypeptides may be a concomitant response at the level of mitochondrial respiration (Wilson et al. 2006). This latter conclusion requires more research since the abundance of *AOX* transcript or protein has not been measured in UWO241 in response to changes in light irradiance.

In summary, the structure and function of *AOX* in UWO241 are clearly dissimilar to those of the related *C. reinhardtii,* and may be a product of the polar environment it inhabits. The current body of evidence showing unique adaptations of UWO241 have mainly focused on its photosynthetic apparatus (Morgan-Kiss et al. 2002; Morgan-Kiss et al. 2005; Pocock et al. 2011; Szyszka et al. 2007), and physiological response to heat stress (Possmayer et al. 2011). These adaptations have suggested unique responses to an ecological niche undergoing

extremely slow rates of change. Examination of the *AOX* from UWO241 has also shown distinct differences in its regulation when compared to that of *C. reinhardtii*. The differences between mesophilic and psychrophilic photoautotrophs observed here highlight the structural and functional divergence of UWO241 and *C. reinhardtii* AOX.

5   Conclusions and Future Directions

From this study it can be concluded that the regulation of UWO241 *AOX1* is not linked to nitrate assimilation as is the case in *C. reinhardtii*. It would be prudent then to examine the location of *AOX* within the UWO241 genome since in the case of *C. reinhardtii* it is located within one of the two NAR gene clusters (Pakkiriswami et al. 2009). This prospect has become more realistic with the recent sequencing of the UWO241 genome (Possmayer et al., personal comm.). With a genome in hand, it may be possible to examine potential transcriptional regulatory regions surrounding UWO241 *AOX1*.

Another direct way of measuring the transcriptional regulation of *AOX* would be to use a hybrid *AOX*/reporter gene such as the arylsulfatase reporter gene (*Ars*) (Molen et al. 2006). Measuring the reporter gene activity under various treatments would shed some light on the biological function of AOX in the context of an Antarctic algal species.

The transcriptional regulation of *AOX* has been linked to many biological processes (see Millenaar and Lambers 2003). It may therefore be prudent to examine the expression of *AOX* under the ecological conditions UWO241 encounters in its stratified layer of water, as outlined by Priscu (1997) and Lizotte and Priscu (1994). This approach would require transformation of UWO241 with an expression vector containing a reporter gene – a technique that has not yet been attempted in UWO241.

Since the measurement of AOX protein accumulation was not possible, an important future direction would be to develop an AOX antibody that can recognize the UWO241 AOX1 polypeptide. The modifications in polypeptides associated with cold adaptation seem to inhibit the recognition of epitopes by antibodies for conserved polypeptides.

It would also be of interest to examine any post-translational modifications that may occur in response to hydrogen peroxide or heat stress. Measurement of this would require an anti-glutathione antibody or additional antibodies capable of recognizing post-translational modifications of isolated AOX protein. One limiting factor that may prevent the development of an AOX antibody is the isolation of AOX protein. This would be possible by cloning the genomic sequence of UWO241 *AOX1* in a prokaryotic vector. This approach

may pose several challenges relating to proper folding of the cold-adapted AOX in a mesophilic bacterial host with an optimal growth temperature of 37°C.

References

Albury MS, Elliott C, and Moore AL (2009). Towards a structural elucidation of the alternative oxidase in plants. Physiologia Plantarum, *137*(4), 316–27.

Andersson ME, and Nordlund P (1999). A revised model of the active site of alternative oxidase. FEBS Letters, *449*(1), 17–22.

Berthold DA, Andersson ME, and Nordlund P (2000). New insight into the structure and function of the alternative oxidase. Biochimica et Biophysica Acta Bioenergetics, *1460*(2), 241.

Brock T, and Freeze H (1969). *Thermus aquaticus* gen. n. and sp. n., a nonsporulating extreme thermophile. Journal of Bacteriology, *98*(I), 289–97.

Brock T. (1985). Life at high temperatures. Science, *230*(4722), 132–38.

Brown GC (2001). Regulation of mitochondrial respiration by nitric oxide inhibition of cytochrome c oxidase. Biochimica et Biophysica Acta, *1504*(1), 46–57.

Castellano I, Ruocco MR, Cecere F, Di Maro A, Chambery A, Michniewicz A, Parlato, G, Masullo M, and De Vendittis E (2008). Glutathionylation of the iron superoxide dismutase from the psychrophilic eubacterium *Pseudoalteromonas haloplanktis*. Biochimica et Biophysica Acta, *1784*(5), 816–26.

Cavicchioli R (2006). Cold-adapted archaea. Nature Reviews Microbiology, *4*(5), 331–43.

Deegenaars ML, and Watson K (1998). Heat shock response in psychrophilic and psychrotrophic yeast from Antarctica. Extremophiles, *2*(1), 41–50.

Devos N, Ingouff M, Loppes R, and Matagne RF (1998). Rubisco adaptation to low temperatures: a comparative study in psychrophilic and mesophilic unicellular algae. Journal of Phycology, *34*(4), 655–60.

Dinant M, Baurain D, Coosemans N, Joris B, and Matagne RF (2001). Characterization of two genes encoding the mitochondrial alternative oxidase in *Chlamydomonas reinhardtii*. Current Genetics, *39*(2), 101.

Dobrota C (2006). Energy dependant plant stress acclimation. Reviews in Environmental Science and Bio/Technology, *5*(2-3), 243–51.

D'Amico S, Marx JC, Gerday C, and Feller G (2003). Activity-stability relationships in extremophilic enzymes. The Journal of Biological Chemistry, *278*(10), 7891–6.

Feller G, Thiry M, and Arpigny J (1990). Lipases from psychrotropic Antarctic bacteria. FEMS Microbiology Letters*, 66*(1-3), 239–43.

Feller G, and Gerday C (2003). Psychrophilic enzymes: hot topics in cold adaptation. Nature Reviews Microbiology, *1*(3), 200–8.

Fernandez E, and Galvan A (2008). Nitrate assimilation in *Chlamydomonas*. Eukaryotic Cell, *7*(4), 555–9.

Finnegan PM, Wooding R, and Day DA (1999). An alternative oxidase monoclonal antibody recognises a highly conserved sequence among alternative oxidase subunits. FEBS Letters, *447*(1), 21–4.

Graf P, and Jakob U (2002). Redox-regulated molecular chaperones. Cellular and Molecular Life Sciences, *59*(10), 1624–31.

Gromoff EDVon, Treier U, and Beck C (1989). Three light-inducible heat shock genes of *Chlamydomonas reinhardtii*. Molecular and Cellular Biology, *9*(9), 3911.

Harris EH (1989) The *Clamydomonas* Sourcebook: A Comprehensive Guide to Biology and Laboratory Use. Academic Press. San Diego.

Jeffrey SW, and Humphrey GF (1975). New spectrophotometric equations for determining chlorophyll a, chlorophyll b, chlorophyll c1 and chlorophyll c2 in higher plants algae and natural phytoplankton. Biochemie und Physiologie der Pflanzen, *167*(2), 191-94.

Kern A, Hartner FS, Freigassner M, Spielhofer J, Rumpf C, Leitner L, Fröhlich KU, and Glieder A (2007). *Pichia pastoris* "just in time" alternative respiration. Microbiology (Reading, England), *153*(Pt 4), 1250–60.

Lizotte M, and Priscu J (1994). Natural fluorescence and quantum yields in vertically stationary phytoplankton from perennially ice-covered lakes. Limnology and Oceanography, *39*(6), 1399–1410.

Margesin R, and Schinner F (1994). Properties of cold-adapted microorganisms and their potential role in biotechnology. Journal of Biotechnology, *33*(1), 1–14.

Maxwell DP, Nickels R, and McIntosh L (2002). Evidence of mitochondrial involvement in the transduction of signals required for the induction of genes associated with pathogen attack and senescence. The Plant Journal: for Cell and Molecular Biology, *29*(3), 269–79.

Maxwell DP, Wang Y, and McIntosh L (1999). The alternative oxidase lowers mitochondrial reactive oxygen production in plant cells. Proceedings of the National Academy of Sciences of the United States of America, *96*(14), 8271–6.

McCabe T, Finnegan P, Harvey Millar A, Day D, and Whelan J (1998). Differential expression of alternative oxidase genes in soybean cotyledons during postgerminative development. Plant Physiology, *118*(2), 675–82.

McDonald A (2009). Alternative oxidase: what information can protein sequence comparisons give us? Physiologia Plantarum, *137*(4), 328.

McDonald AE, Vanlerberghe GC, and Staples JF (2009). Alternative oxidase in animals: unique characteristics and taxonomic distribution. The Journal of Experimental Biology, *212*(Pt 16), 2627–34.

Meeuse B (1975). Thermogenic respiration in aroids. Annual Review of Plant Physiology, *26*(83), 117–26.

Metpally RPR, and Reddy BVB (2009). Comparative proteome analysis of psychrophilic versus mesophilic bacterial species: Insights into the molecular basis of cold adaptation of proteins. BMC Genomics, *10*, 11.

Millenaar FF, and Lambers H (2003). The Alternative Oxidase: in vivo regulation and function. Plant Biology, *5*(1), 2–15.

Mittler R, Vanderauwera S, Gollery M, and Van Breusegem F (2004). Reactive oxygen gene network of plants. Trends in Plant Science, *9*(10), 490–8.

Molen TA, Rosso D, Piercy S, and Maxwell DP (2006). Characterization of the alternative oxidase of *Chlamydomonas reinhardtii* in response to oxidative stress and a shift in nitrogen source. Physiologia Plantarum, *127*(1), 74–86.

Morgan-Kiss R, Ivanov A, and Williams J (2002). Differential thermal effects on the energy distribution between photosystem II and photosystem I in thylakoid membranes of a psychrophilic and a mesophilic alga. Biochimica et Biophysica Acta, *1561*(2), 251-65.

Morgan-Kiss RM, Ivanov AG, Pocock T, Krol M, Gudynaite-Savitch L, and Hüner NPA (2005). The Antarctic psychrophile, *Chlamydomonas raudensis* Ettl (UWO241) (*Chlorophyceae, Chlorophyta*), exhibits a limited capacity to photoacclimate to red light. Journal of Phycology, *41*(4), 791–800.

Morgan-Kiss R, Ivanov A, and Hüner N (2002). The Antarctic psychrophile, *Chlamydomonas subcaudata*, is deficient in state I-state II transitions. Planta, *214*(3), 435–45.

Morgan-Kiss R, Priscu J, Pocock T, Gudynaite-Savitch L, Hüner NPA (2006). Adaptation and acclimation of photosynthetic microorganisms to permanently cold environments. Microbiology and Molecular Biology Review, *70*(1), 222.

Morita RY (1975). Psychrophilic bacteria. Bacteriological Reviews, *39*(2), 144–67.

Neale PJ, and Priscu JC (1995). The photosynthetic apparatus of phytoplankton from a perennially ice-covered antarctic lake: acclimation to an extreme shade environment. Plant Cell Physiology, *36*(2), 253-63.

Noctor G, De Paepe R, and Foyer CH (2007). Mitochondrial redox biology and homeostasis in plants. Trends in Plant Science, *12*(3), 125–34.

Pakkiriswami S, Beall BFN, and Maxwell DP (2009). On the role of photosynthesis in the nitrate-dependent induction of the alternative oxidase in *Chlamydomonas reinhardtii*. Botany, *87*(4), 363–74.

Pikuta EV, Hoover RB, and Tang J (2007). Microbial extremophiles at the limits of life. Critical Reviews in Microbiology, *33*(3), 183–209.

Pocock T, Lachance MA, Proeschold T, Priscu JC, Kim SS, and Hüner NPA (2004). Identification of a psychrophilic green alga from Lake Bonney Antarctica: *Chlamydomonas raudensis* Ettl. (UWO 241) *Chlorophyceae*. Journal of Phycology, *40*(6), 1138–48.

Pocock T, Vetterli A, and Falk S (2011). Evidence for phenotypic plasticity in the Antarctic extremophile *Chlamydomonas raudensis* Ettl. UWO 241. Journal of Experimental Botany, *62*(3), 1169–77.

Possmayer M, Berardi G, Beall BFN, Trick CG, Hüner NPS, and Maxwell DP (2011). Plasticity of the psychrophilic green alga *Chlamydomonas raudensis* (UWO 241) (*Chlorophyta*) to supraoptimal temperature stress. Journal of Phycology, *47*(5), 1098–109.

Priscu J (1997). The biogeochemistry of nitrous oxide in permanently ice-covered lakes of the McMurdo Dry Valleys, Antarctica. Global Change Biology, *3*(4), 301–15.

Quesada A, Hidalgo J, and Fernández E (1998). Three Nrt2 genes are differentially regulated in *Chlamydomonas reinhardtii*. Molecular and General Genetics, *258*(4), 373–7.

Raymond J, Sullivan C, and DeVries A (1994). Release of an ice-active substance by Antarctic sea ice diatoms. Polar Biology, *14*(1), 71–5.

Rothschild LJ, and Mancinelli RL (2001). Life in extreme environments. Nature, *409*(6823), 1092–101.

Russell N (1997). Psychrophilic bacteria—molecular adaptations of membrane lipids. Comparative Biochemistry and Physiology, *118A*(3), 489-93.

Russell NJ (1990). Cold adaptation of microorganisms. Philosophical Transactions of the Royal Society of London. Series B: Biological Sciences, 326(1237), 595–608.

Russell RJ, Gerike U, Danson MJ, Hough DW, and Taylor GL (1998). Structural adaptations of the cold-active citrate synthase from an Antarctic bacterium. Structure, *6*(3), 351–61.

Sambrook J, and Russell DW (2001). Molecular Cloning: A Laboratory Manual (Vol. 3, p. A8.19). Cold Spring Harbor, N.Y.: Cold Spring Harbor Laboratory Press.

Siddiqui KS, and Cavicchioli R (2006). Cold-adapted enzymes. Annual Review of Biochemistry, *75*, 403–33.

Siedow J, and Berthold D (1986). The alternative oxidase: a cyanide resistant respiratory pathway in higher plants. Physiologia Plantarum, *66*, 569–74.

Siedow J, and Moore A (1993). A kinetic model for the regulation of electron transfer through the cyanide-resistant pathway in plant mitochondria. Biochimica et Biophysica Acta -Bioenergetics, *1142*, 165–74.

Sueoka N (1960). Mitotic replication of deoxyribonucleic acid in *Chlamydomonas reinhardtii*. Proceedings of the National Academy of Sciences of the United States of America, *46*, 83–91.

Sweetlove LJ, Heazlewood JL, Herald V, Holtzapffel R, Day DA, Leaver CJ, and Millar AH (2002). The impact of oxidative stress on Arabidopsis mitochondria. The Plant Journal: for Cell and Molecular Biology, *32*(6), 891–904.

Szyszka B, Ivanov AG, and Hüner NPA (2007). Psychrophily is associated with differential energy partitioning, photosystem stoichiometry and polypeptide phosphorylation in *Chlamydomonas raudensis*. Structure and Function of Photosystems, *1767*(6), 789–800.

Thompson JD, Gibson TJ, Plewniak F, Jeanmougin F, Higgins DG (1997) The ClustalX windows interface: flexible strategies for multiple sequence alignment aided by quality analysis tools. Nucleic Acids Research, *24,* 4876–82

Tubea B, Hawxby K, and Mehta R (1981). The effects of nutrient, pH and herbicide levels on algal growth. Hydrobiologia, *79*(3), 221–7.

Untergasser A. "RNA Miniprep using CTAB" Untergasser's Lab. Summer 2008. (Accessed Sept. 2011).
<http://www.untergasser.de/lab/protocols/miniprep_rna_ctab_v1_0.htm>.

Umbach AL, and Siedow JN (1993). Covalent and noncovalent dimers of the cyanide-resistant alternative oxidase protein in higher plant mitochondria and their relationship to enzyme activity. Plant Physiology, *103*(3), 845–54.

Vanlerberghe GC, and McIntosh L (1997). Alternative oxidase: from gene to function. Annual Review of Plant Physiology and Plant Molecular Biology, *48*, 703-34.

Vanlerberghe G, and McIntosh L (1992). Lower growth temperature increases alternative pathway capacity and alternative oxidase protein in tobacco. Plant Physiology, *100*(1), 115–9.

Vayda ME, and Yuan ML (1994). The heat shock response of an antarctic alga is evident at 5 degrees C. Plant Molecular Biology, *24*(1), 229–33.

Voytek M, Priscu J, and Ward B (1999). The distribution and relative abundance of ammonia-oxidizing bacteria in lakes of the McMurdo Dry Valley, Antarctica. Hydrobiologia, *138*, 113–30.

Wan XY, and Liu JY (2008). Comparative proteomics analysis reveals an intimate protein network provoked by hydrogen peroxide stress in rice seedling leaves. Molecular and Cellular Proteomics, *7*(8), 1469–88.

Wilson KE, Ivanov AG, Öquist G, Grodzinski B, Sarhan F, and Hüner NPA (2006). Energy balance, organellar redox status, and acclimation to environmental stress. Canadian Journal of Botany, *84*(9), 1355–70.

Yoshida K, Terashima I, and Noguchi K (2007). Up-regulation of mitochondrial alternative oxidase concomitant with chloroplast over-reduction by excess light. Plant and Cell Physiology, *48*(4), 606–14.

Zecchinon L, Claverie P, Collins T, D'Amico S, Delille D, Feller G, Georlette D, Gratia E, Hoyoux A, Meuwis MA, Sonan G, Gerday C (2001). Did psychrophilic enzymes really win the challenge? Extremophiles, *5*(5), 313–21.

Appendices
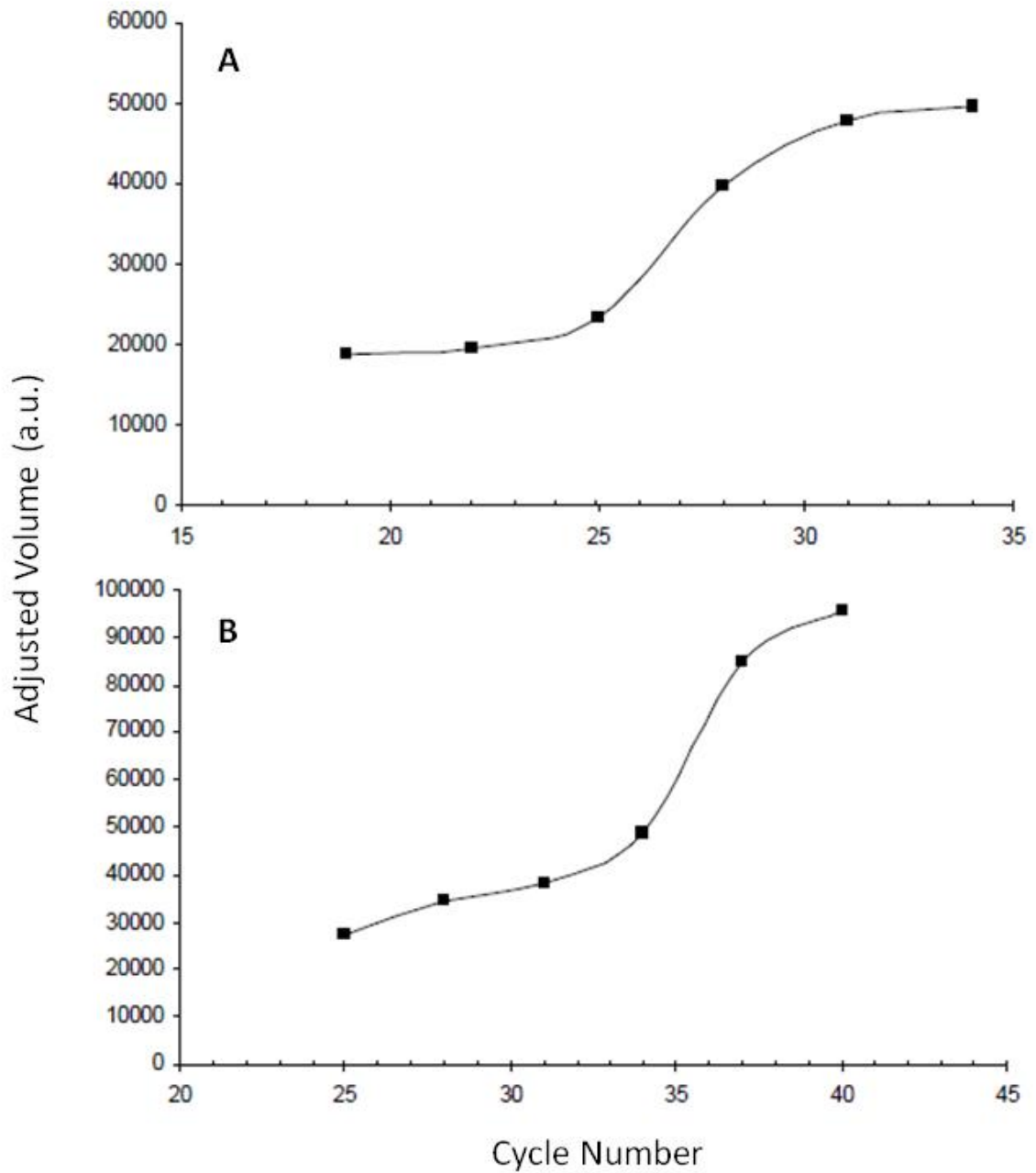
Appendix A PCR cycle number optimization of primers for large subunit rDNA (A) and *AOX* (B) in a reverse transcribed reaction from nitrate treated *Chlamydomonas sp.* UWO241.

```
        1        10            20            30            40            50            60            70            80            90           100
TCGAAATTAACCCTCACTAAAGGGAACAAAAGCTGGAGCTCCACCGCGGTGGCGGCCGCTCTAGAACTAGTGGATCCCCCGGGCTGCAGGATCGCNAAGTTTATTCTTG

      110           120           130           140           150           160           170           180           190           200           210
TTTCGTCCAGGTCATCAACCTTGGTCCCAAACAACCGCCCTTGCGTGCCAGAGAGCCCGCACTAACGCGAGCCGCAACTTCGCTTTTCCGACACCACCATGCTTCGGCT

      220           230           240           250           260           270           280           290           300           310           320
CCTCTCTGCGCGCGCCGCCCGCGCTGTGCAGCACACCAACCTGTCATCCCTCCCGGCTGCCCTGGCCCAGCCCGCTAGTGGCGATGCGCTGATCCCAGGATGGAGCCAG

      330           340           350           360           370           380           390           400           410           420           430
GCGCGCTCCCCCTTTTCGTCGCTTCCGGGCTCTGGCGCCCACCACATGCCGCTGCTGACCGGCAGCTGGGACGAGCGCGAGCAGGCCAAGGCGCAGGGGGCTCGCCAGC

      440           450           460           470           480           490           500           510           520           530           540
ACCAGCTGCTGTCTGGGTTTGCGAAGCTTGCGTCTGAGCAGAAGGTGGAGCTGCATCCGGGCATGAAGAAGCAGCAGGTGATGGCAGGCGCGCTCGAGCCCACCGAGTG

      550           560           570           580           590           600           610           620           630           640           650
GACCTGGGGCGACCGGTCGTACACTGCAGAGTACATGGAGAGCCTGAAGCCCATGCACAAGCCGCCGGTCACGTTCACCGAGAAGATGGCGTACTGGGCGATCCAGGGC

      660           670           680           690           700           710           720           730           740           750           760
ACCCGCGCCTCCTTCGACTGGGTCACCAGCTACAAGCATGACGTGCCCCAGTCCGAGGCCCAGTGGCTCCGACGCATCGTGTTCCTCGAGACCGTCGCCGGGGTGCCCG

      770           780           790           800           810           820           830           840           850           860           870
GCATGGTCGGCGGCGTGCTGCGCCACCTGCGCTCGCTGCGCCTGATGAAGGCGGACAAGGGCTGGATCGGCTCGCTGCTCGAGGAGGCCGAGAACGAGCGCATGCACCT

      880           890           900           910           920           930           940           950           960           970           980
GCTGGTCTTCCTGCAGATGCGCCAGCCCGAGTGGTACTTCAAGGCAGCGGTCCTGATCGCCCAGGGCGTCTACTGGAACGTCTTCTTCCTCTCCTACCTGATGGCCCCC

      990         1,000         1,010         1,020         1,030         1,040         1,050         1,060         1,070         1,080         1,090
AAGTTCTGCCACGCCGTCGTTGGGTACCTCGAGGAGGAGGCCGTCCGCACGTACACTCACCTTATTGAGGACATCGACGCCGGTCACGTTTGGAAGGACCAGAAGCCGC

     1,100         1,110         1,120         1,130         1,140         1,150         1,160         1,170         1,180         1,190
CGCCGATCGCCATCACCTACTGGCACCTGGGCGAGAACGCGACCATGCGCGACCTGGCACTGGCCGTCCGCGCCGACGAGGCGTCGCACTCGCACGTGAACCACAAGCT

     1,200         1,210         1,220         1,230         1,240         1,250         1,260         1,270         1,280         1,290         1,300
GAGCGAGACCGCCCAGGACGCGCCCAACCCGTTCATGGTCGTCAAGGGCGGCTCTGTCAACACCAAGGAGATGCTCTGAACGCAGCACCCTGGAGCGTCCGTTTGAGTG

     1,310         1,320         1,330         1,340         1,350         1,360         1,370         1,380         1,390         1,400         1,410
AAGTGAGCACGCTGTCCGGTCCACACCAAACGGTGTGGACAGGTATGAACAAGTACCAAGGCCCACACTTGGGGTGCCTGTCGTAACACCGCAGTCGACCGGTTGATTG

     1,420         1,430         1,440         1,450         1,460         1,470         1,480         1,490         1,500         1,510       1,522
GGAACGCGCAACGGGCTCCGTCCCCCGACCCGTTGAAACCTGGGCGGCGCTCGGCCGGTACATCTGCTTATTGATTATCCCGCAGGCGGCCGACCGGCTGGTGGA
```

Appendix B The full cDNA sequence of *Chlamydomonas sp.* UWO241 *AOX1.*

Sequence data was amplified from a cDNA library through PCR using two vector specific and two gene specific primers. Black bars show the site of recognition for the gene specific primers. Grey bar shows the 317 bp area of overlap used to orient the two gene fragments to construct a full sequence.
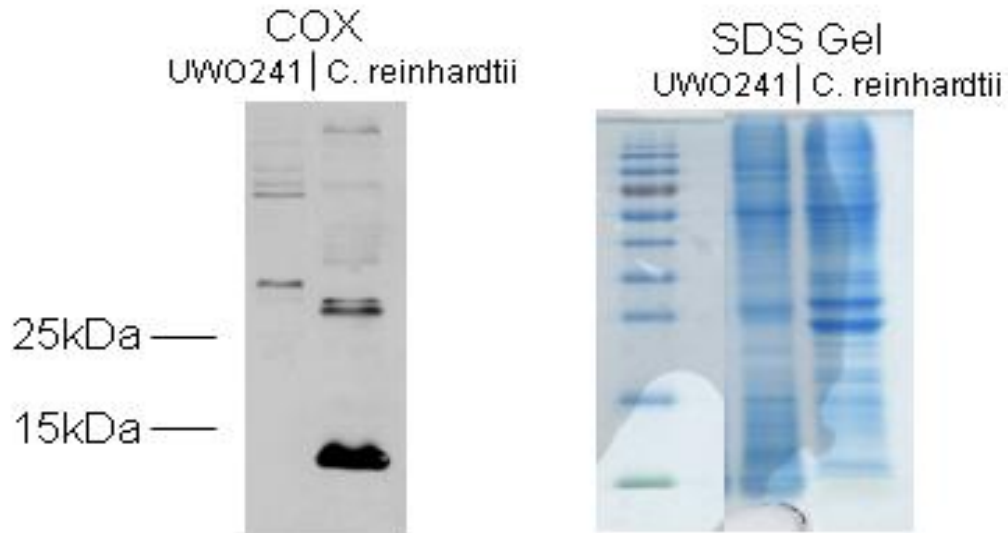
Appendix C Immunoblotting with Cytochrome oxidase (COX) antibody raised in *C. reinhardtii* shows no cross reactivity in total protein samples from *Chlamydomonas sp.* UWO241 (left figure labeled 'COX').

Expected banding patterns for *C. reinhardtii* were located at approximately 14 kDa. High molecular banding patterns observed are considered non-specific binding. Both UWO241 and *C. reinhardtii* 325R cells were grown under nitrate conditions and total protein was separated via SDS-PAGE (right figure labeled 'SDS Gel'). Resulting gels were stained with coomassie blue to show protein migration (stained protein standard ladder shown indicating molecular mass in kDa with the lowest band representing 10 kDa).

Curriculum Vitae

Name: Michael Inman

Post-Secondary Western University
Education and   London, Ontario, Canada
Degrees: 2005-2010 Honors B.Sc.

        Western University
        London, Ontario, Canada
        2010-2013 M.Sc.

Scholarships: Graduate Research Scholarship
        Western University
        2010/09- 2012/08

Related Work   Teaching Assistant
Experience   Western University
        2010/09- 2013/04